Continuous succinic acid fermentation using immobilised *Actinobacillus succinogenes*

by Karishma Maharaj

Dissertation presented in partial fulfilment of the requirements for the degree of

Master of Engineering in Chemical Engineering

Faculty of Engineering, the Built Environment and Information Technology,
Department of Chemical Engineering,
University of Pretoria

Supervisor: Prof. W. Nicol

November 2013

Synopsis

Actinobacillus succinogenes cells were grown on Poraver® support particles in a packed-bed reactor. Dilution rates (D) of 0.054–0.72 h^{-1} were investigated. Glucose was used as substrate. CO_2 (g) was bubbled into a complex medium to satisfy the fixation requirements and maintain anaerobic conditions. At D ≥ 0.31 h^{-1}, an initial glucose concentration of 35 $g.L^{-1}$ was used; at lower dilution rates, this was increased to 60 $g.L^{-1}$ in order to avoid substrate limitations. By-product formation included acetic and formic acids. A maximum productivity of 10.7 $g.L^{-1}$ was obtained at D = 0.7 h^{-1}.

It was found that the system provided repeatable results at a given D. The longest steady state period was maintained for about 97 h at D = 0.31 h^{-1}. Steady state stability was maintained for > 72 h at D < 0.31 h^{-1}. For periods longer than 75 h, however, inhibitory acid titres resulted in a gradual decline in productivity. At higher dilution rates, long-term stability could not be maintained. The low acid titres produced significant biofilm sloughing following aggressive biofilm growth, resulting in oscillatory system behaviour.

For fermentation times < 115 h, the dilution rate was secondary to the attachment area in determining the total biomass at steady state. Total biomass values were then used to determine specific rates. A clear trend was observed, with the specific glucose consumption rate, and specific acid production rates, increasing with increasing D. This was explained by assuming a maintenance-driven system at all Ds studied.

A product analysis indicated that at ΔS < 15 $g.L^{-1}$, pyruvate formate lyase was the preferred oxidative route. A shift to the pyruvate dehydrogenase pathway occurred at higher ΔS values, so that the highest Y_{SS} values obtained exceeded 0.85 $g.g^{-1}$. A decrease in C3 by-product formation resulted in high Y_{SS} values being maintained, indicating an additional, unknown source of nicotinamide adenine dinucleotide (NADH).

It is recommended that any process utilising immobilised *A. succinogenes* cells should operate at an intermediate D, in order to maintain long-term reactor stability, high productivities and good yields.

Keywords: Succinic acid; *Actinobacillus succinogenes*; Continuous fermentation; Biofilm; Pyruvate formate lyase; Pyruvate dehydrogenase

Acknowledgements

The financial assistance of the National Research Foundation (DAAD-NRF) towards this research is hereby acknowledged. Opinions expressed and conclusions arrived at, are those of the author and are not necessarily to be attributed to the DAAD-NRF.

Contents

List of Figures

List of Tables

Nomenclature

A_a	Poraver® mass before fermentation	g
A_b	Poraver® mass after fermentation	g
C_{SA}	Succinic acid concentration	$g.L^{-1}$
D	Dilution rate based on total volumetric flow	h^{-1}
DCW_{vial}	Dry cell weight present in vial	g
d_p	Support particle diameter	mm
FA/AA	Formic acid on acetic acid mass ratio	$g.g^{-1}$
K_{is}	Inhibiting substrate concentration	$g.L^{-1}$
K_{mp}	Product-associated maintenance constant	$g.L^{-1}$
K_{ms}	Substrate-associated maintenance constant	$g.L^{-1}$
K_s	Substrate-associated Monod constant	$g.L^{-1}$
m_p	Product-associated maintenance	h^{-1}
M_p	Product-associated maintenance (substrate-dependent)	h^{-1}
m_s	Substrate-associated maintenance	h^{-1}
M_s	Substrate-associated maintenance (substrate-dependent)	h^{-1}
p_{max}	Maximum inhibitory succinic acid concentration	$g.L^{-1}$
$p_{i,max}$	Maximum inhibitory concentration of component i	$g.L^{-1}$
P_{SA}	Succinic acid productivity	$g.L^{-1}.h^{-1}$
q_i	Volumetric production rate of component i	$g.L^{-1}.h^{-1}$
r_i	Specific production of component i (based on dry cell weight measurements)	h^{-1}

SA/AA	Succinic acid on acetic acid mass ratio	$g.g^{-1}$
ΔS	Glucose consumed	$g.L^{-1}$
S	Reactor substrate concentration	$g.L^{-1}$
S_o	Initial substrate concentration in feed	$g.L^{-1}$
$S_{o,adj}$	Initial substrate concentration entering reactor	$g.L^{-1}$
V	Working reactor volume	mL
$V_{collection\ volume}$	Volume of biomass collection bottle	L
X_{tot}	Total biomass	$g.L^{-1}$
x	Suspended cell concentration	$g.L^{-1}$
Y_{SA}	Acetic acid yield on substrate	$g.g^{-1}$
Y_{SF}	Formic acid yield on substrate	$g.g^{-1}$
Y_{SS}	Succinic acid yield on substrate	$g.g^{-1}$
Y_{xs}^{true}	True substrate on biomass mass ratio	$g.g^{-1}$
Y_{xp}^{true}	True product on biomass mass ratio	$g.g^{-1}$
Y_{sx}^{obs}	Observed biomass yield on substrate	$g.g^{-1}$

Greek

γ	Substrate conversion	$g.g^{-1}$
μ_{max}	Maximum specific growth rate	h^{-1}
μ	Specific growth rate	h^{-1}

Abbreviations

AA	acetic acid
AAD	absolute average deviation
ATP	adenosine triphosphate

DAQ	data acquisition
EPS	extracellular polysaccharides
FA	formic acid
HFBR	hollow fibre bioreactor
HPLC	high-performance liquid chromatography
NADH	nicotinamide adenine dinucleotide
PDH	pyruvate dehydrogenase
PEP	phosphoenolpyruvate
PFL	pyruvate formate lyase
PTFE	polytetrafluoroethylene
RID	refractive index detector
SA	succinic acid
TCA	tri-carboxylic acid
TBQ	total biomass quantification
TSB	tryptone soy broth

Chapter 1 Introduction

The world's dependence on fossil resources has led to dwindling coal, gas and oil reserves. The chemical and energy industries have therefore seen an increase in costs associated with the use of these non-renewables. Furthermore, global warming has resulted in a shift by government and industry towards more eco-friendly processes. These factors have generated significant interest in the prospects of a bio-based industry. The concept of a "biorefinery", in which biofuels are produced alongside lower-volume, high-value chemicals, presents a highly attractive, integrated approach to bioprocessing (Sauer *et al.,* 2008). Nature offers an abundant supply of biomass as feedstock for energy and chemical production. However, conversion technologies are still in their infancy, making such processes more expensive than well-established, petroleum-based routes. Nevertheless, the urgent need for alternatives to the industry status quo has driven research into the development of economically feasible bioprocesses (Bechthold *et al.*, 2008; McKinlay *et al*., 2007; Zeikus *et al*., 1999; Sauer *et al.*, 2008; Cukalovic & Stevens, 2008).

Organic acids, in particular, have been identified as potential bio-based platform chemicals. Their functional groups allow for further processing into a variety of products. Many of these organic acids can be derived via microbial fermentation, in which carbohydrates are converted into biomass and metabolic products. Succinic acid is one such product, considered to be of huge economic value in the future (Sauer *et al.*, 2008; Bechthold *et al.*, 2008). Transparency Market Research (Mynewsdesk, 2013) recently reported that the market for succinic acid and its immediate derivatives would reach 250 kt/a by 2018, translating into US$ 836 million. These derivatives include commodity chemicals, such as tetrahydrofuran, gamma-butyrolactone, 1,4-butanediol, adipic acid and various pyrrolidones (Zeikus *et al.*, 1999; Bechthold *et al.*, 2008; Sauer *et al.*, 2008; Cukalovic & Stevens, 2008). Succinic acid-derived polymers may also compete for a share of the booming polymer industry – a market that is projected to reach US$ 567

billion by 2017 (Lucintel, 2012). Many companies have already begun to capitalise on the growing succinic acid market. Myriant, BioAmber, Reverdia and a collaboration between BASF and CSM have all seen pilot plant successes, with commercial production facilities almost or already complete (Bastidon, 2012).

Currently, most bioprocesses, as used in the pharmaceutical and food industries, are concerned with the production of low-volume, high-value products. This makes the use of batch fermentation a favoured choice. However, batch processing involves long, non-productive periods associated with emptying, cleaning, refilling and sterilising. Exponential growth, in which biomass formation competes with metabolite production for the carbon source, is often the most important production phase in batch fermentation. Continuous processing is necessary if succinic acid is to become a high-demand platform chemical. Not only will production volumes be higher, but continuous processing will allow better process control and efficiency. Continuous processing also allows long periods of preferential metabolite production during the stationary phase (Tampion & Tampion, 1987: 184–186).

Bacteria usually produce biofilms under conditions of stress. Cells are surrounded by a strong, sticky network of extracellular polysaccharides (EPS), which keeps them attached to a surface. Within the biofilm are interstices, used for the transport of nutrients and metabolic wastes (Sutherland, 2001). Biofilms are the result of self-immobilisation. The presence of a suitable substratum within a reactor may result in the adsorption of self-immobilising cells, such as *A. succinogenes*, effectively increasing the cell density. This increase in cell density is often associated with higher volumetric productivities when compared with free cell systems. Immobilised cells also possess better thermal, chemical, shear force-resistant and growth inhibition characteristics (Galaction *et al.*, 2012). The stationary phase in the life cycle of a bacterium is often associated with higher product yields as the carbon flux towards biomass production is negligible. Carbon is used primarily for metabolite production in order to produce the energy required for maintenance processes. The stationary phase of an immobilised cell is much longer than that of free cells. This implies that a longer period of maintenance-driven metabolite production is exhibited by immobilised cells (Sarika *et al.*, 2012).

The available literature on succinic acid production is widely varied, utilising several types of substrate, reactor configurations and microorganisms. Some of the more well-studied biocatalysts include *Actinobacillus succinogenes*, *Anaerobiospirullum succiniproducens*, recombinant *Escherichia coli* (Jantama *et al.*, 2008; Sánchez *et al.*, 2005; Vemuri *et al*., 2002), and *Mannheimia succiniproducens* (Beauprez *et al.*, 2010; Samuelov *et al.*, 1991). *A. succinogenes* is a natural producer of succinic acid under anaerobic conditions. It has been well researched, is known for producing high acid titres and can ferment a wide variety of substrates, including glucose, fructose, arabinose and xylose. The bulk of the available literature concerns batch studies. Of the few continuous studies, most were performed using a chemostat. Mwakio (2012), Van Heerden (2012) and Urbance *et al.* (2004) performed continuous runs using immobilised *A. succinogenes*. Since *A. succinogenes* is a natural biofilm producer, it is almost impossible to realise ideal chemostat conditions. Kim *et al.* (2009) and Meynial-Salles *et al.* (2008) implemented cell recycling in continuous systems, the former using *A. succinogenes* and the latter *A. succiniproducens*. Kinetic studies on succinic acid producers are limited and on *A. succinogenes* they are even more so. Corona-González *et al.* (2008) and Lin *et al.* (2008) performed a kinetic analysis on suspended *A. succinogenes* using batch runs. Lee *et al*. (2009) conducted a continuous kinetic study on free *A. succiniproducens,* while Li *et al.* (2010) used *A. succinogenes* and *E. coli* in batch runs. There is a clear need for research into continuous succinic acid production using immobilised cells, with particular focus on the kinetics and associated reactor performance.

The aim of this research was to investigate continuous, anaerobic succinic acid production, using immobilised *A. succinogenes* cells. A steady state analysis was to be performed, assessing repeatability at a given dilution rate, as well as reactor stability. This study was also directed at gaining insight into the system kinetics. The most important step in this process would be to obtain accurate total biomass measurements. Lastly, product distributions were to be analysed in order to gain insight into metabolic fluxes.

Succinic acid was produced using glucose as the primary carbon source, CO_2 (g), mineral salts, yeast extract and corn steep liquor. Poraver® support particles were

used in a novel packed-bed reactor with recycle. The temperature and pH were controlled at 37 $^{\circ}$C and 6.8 respectively. Dilution rates of 0.054 h^{-1} to 0.72 h^{-1} were tested. At low dilution rates (<0.31 h^{-1}), an initial glucose concentration of 60 $g.L^{-1}$ was used in order to prevent substrate limitation. This was decreased to 35 $g.L^{-1}$ at higher dilution rates.

Chapter 2 Literature survey

2.1 Bio-based Chemicals

Coal, gas and oil have driven industry for the past 150 years. From heat and power generation to chemical production, these non-renewables have served as the backbone of modern civilization. However, the finite nature of fossil resources, and their current consumption rates, would result in the depletion of existing reserves within the next century. As stocks of these raw materials dwindle, their market prices escalate. Furthermore, climate change as a result of greenhouse gas emissions can be attributed largely to the industrial status quo. These issues have produced an interest by governments and industry in bio-based resources. A bio-based industry would lead to the production of fuels and chemicals from biomass effectively replacing current petroleum-derived equivalents. The concept of a “bio-refinery” has become particularly attractive since it would serve to produce high-volume, lower-value biofuels in parallel with lower-volume, high-value chemicals. This integrated approach improves the economic feasibility of individual bio-based processes. (Bechthold *et al.*, 2008; McKinlay *et al.*, 2007; Zeikus *et al.*, 1999; Sauer *et al.*, 2008).

Nature offers an abundant supply of various types of biomass. Plants, in particular, are capable of fast biomass building with minimal human intervention. However, a lack of conversion technology has kept this vast repository hitherto untapped, save for a few niche industries, including paper, biofuels and wood processing. Other stumbling blocks include locally available biomass types, product isolation and purification, and the overall process cost. Petrochemical processes utilise well-established technologies, while bio-based processing is still in its infancy, making the former the cheaper option. Nevertheless, the urgent need to create a sustainable global chemical industry has driven research into the development of economically feasible bioprocesses. Bio-based and petrochemical processes are compared in Table 2.1 (Bechthold *et al.*, 2008; Cukalovic & Stevens, 2008).

Table 2.1: *Comparison of bio-chemical and petrochemical processes (Cukalovic & Stevens, 2008)*

	Production method	
	Petrochemical	***Bio-chemical***
Origin	Non-renewable feedstocks	Renewable feedstocks – carbohydrates
Price considerations	Still cheaper than renewable resources	Downstream processing much more expensive than feedstocks
Routes	Developed routes; established technology	Routes under constant improvement; young technology
Yields and productivity	Generally high	Significant amounts of by-products are common; diluted media; long reaction times
Major disadvantages	High energy demands (pressure and temperature); catalyst disposal problems	Sensitive microorganisms; complex additional nutrients often needed; complicated product recovery; large amounts of waste
Public awareness	Decreasing popularity	Increased interest

Organic acids, in particular, have been identified as potential bio-based platform chemicals, because their functional groups allow for further processing into a wide array of intermediates and end-products. These organic acids are usually the result of expensive oxidative processes, which introduce the functional group to crude-oil-derived hydrocarbons. Carbohydrates already containing these functional groups can be converted into organic acids by fermentation. This is the process by which microbes utilise carbohydrates for growth and other cellular activities, while producing organic compounds as by-products of metabolism (Sauer *et al.*, 2008; Bechthold *et al.*, 2008).

2.2 Succinic Acid: Current and Future Markets

Succinic acid ($HO_2C(CH_2)_2CO_2H$), also known as butanedioic acid, 1,2-ethanedicarboxylic acid or amber acid, is a saturated dicarboxylic acid. Its important properties are shown in Table 2.2, while its structure can be seen in Figure 2.1.

Table 2.2: *Properties of succinic acid (Perry* et al.*, 1997: 2–45)*

Succinic acid properties	***Details***	***Value***	***Units***
Formula	$C_4H_6O_4$		
Acidity	pK_{a1}	4.21	-
	pK_{a2}	5.64	-
Boiling point		235	$^{\circ}C$
Melting point		189	$^{\circ}C$
Molar mass		118.09	$g.mol^{-1}$
Specific gravity		1.57	$g.cm^{-3}$

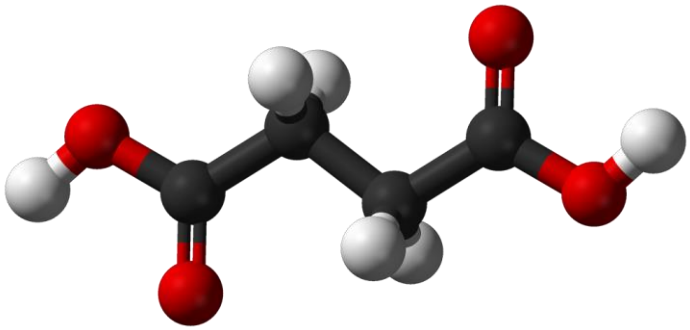

Figure 2.1: *Ball-and-stick model of succinic acid*

At present, the bulk of succinic acid is produced petrochemically by first oxidising N-butane/butadiene to form maleic anhydride. Hydrolysis then converts maleic anhydride to maleic acid, which is thereafter hydrogenated to produce succinic acid

(Cukalovic & Stevens, 2008; Bechthold *et al.*, 2008; Van Heerden, 2012). Until recently, only a small amount of succinic acid, required for the food and pharmaceutical industries, was produced by microbial fermentation (Zeikus *et al.*, 1999).

Succinic acid has the potential to become a bulk-produced platform chemical, serving as an important intermediate. It could replace several petrochemically derived commodity chemicals, particularly those currently synthesised from benzene, such as maleic anhydride (Zeikus *et al.*, 1999; Cukalovic & Stevens, 2008). The resulting products would be much "greener" in both processing and consumption. However, the current succinic acid market is small, being between 30 and 50 kt/a (Higson, 2013). Most succinic acid is used as a surfactant, detergent or foaming agent. It is used in the food industry as a flavouring agent, starch modifier, acidulant or anti-microbial agent. Its health-related uses include the production of pharmaceuticals, antibiotics, amino acids and vitamins. Lastly, it can be used as an ion chelator, and for the manufacture of solvents, synthetic resins and coatings, dyes, photographic chemicals, lacquers, plasticisers, electrolytic bath additives and biodegradable plastics (Zeikus *et al.* 1999; Sauer *et al.*; 2008; Urbance *et al.*, 2003). With its wide range of applicability, it is clear that the potential market for succinic acid is large. A recent report by Transparency Market Research (Mynewsdesk, 2013) projects that the succinic acid market will reach US$ 836 million by 2018, growing at a compound annual rate of 19.4%. It is estimated that about 250 kt/a of succinic acid and its immediate derivatives will be in demand by 2018. These immediate derivatives include commodity chemicals such as tetrahydrofuran, gamma-butyrolactone, 1,4-butanediol, adipic acid and various pyrrolidones. A few of the more notable succinic acid derivatives are shown in Figure 2.2 (Van Heerden, 2012). It is projected that the polymer industry will offer a further US$ 567 billion market to be capitalised upon by 2017 (Lucintel, 2012).

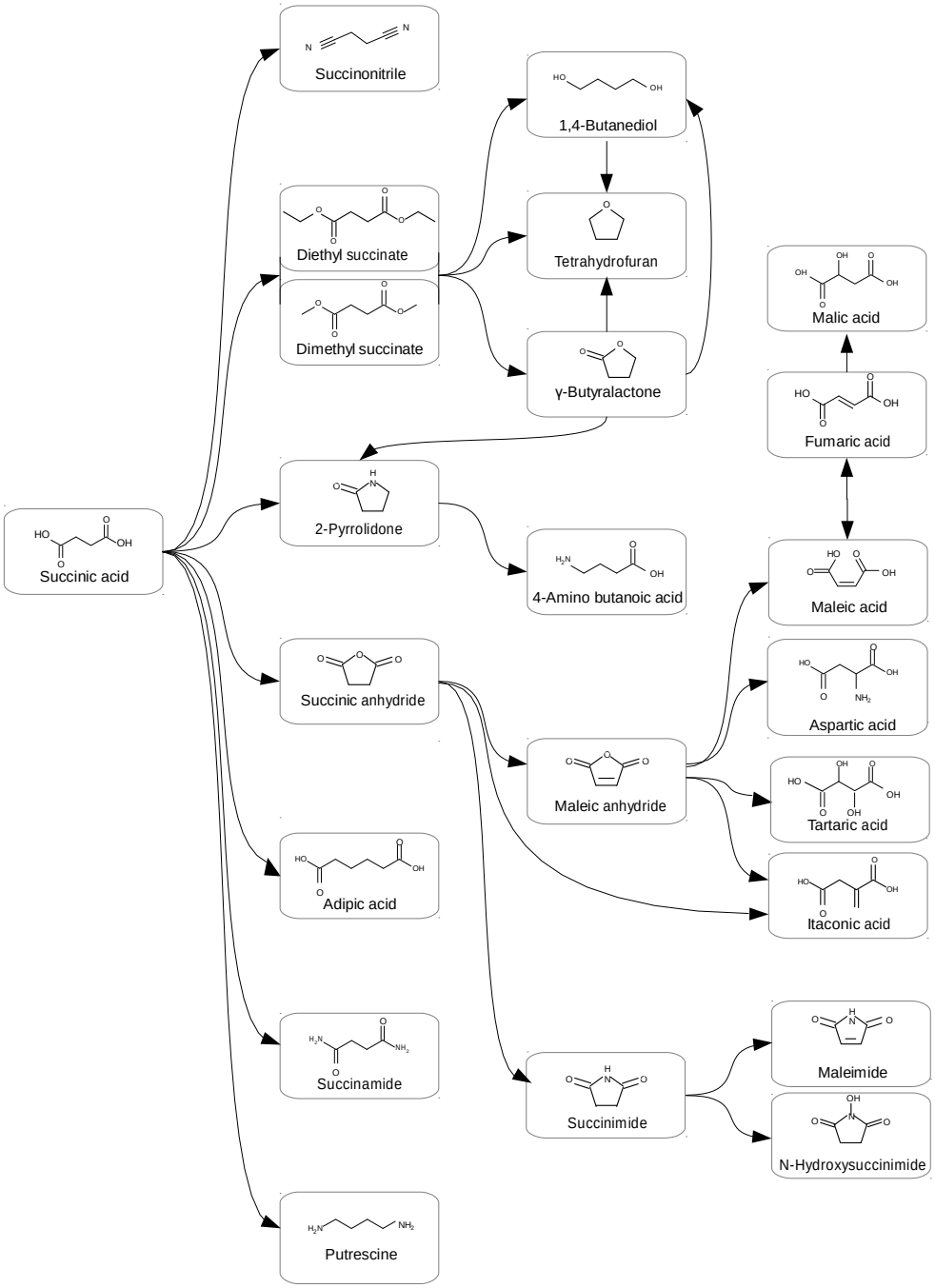

Figure 2.2: *Succinic acid and a few of its economically important derivatives (not all pathways are shown) (Van Heerden, 2012)*

There are several problems with current succinic acid fermentation techniques. Homo-succinic acid production is difficult to achieve. In addition, several strains of succinic acid-producing bacteria exhibit low acid tolerances. Most succinic acid fermentations also occur under anaerobic conditions, which are associated with slow growth. Other stumbling blocks include the cost of downstream processing, complex and expensive nutrient sources, and the dissociation of the produced acid under near-neutral culture conditions (Sauer *et al.*, 2008, Zeikus *et al.*, 1999, McKinlay *et al.*, 2007, Bechthold *et al.*, 2008). These issues have affected the economic feasibility of succinic acid as a commodity chemical. Succinic acid has a current market price of US$ 6–9/kg, making succinate-derived chemicals much more expensive than petrochemicals (Higson, 2013; Geraili *et al.*, 2013). However, many companies have started to tackle the current technological challenges in a race to dominate a potential billion-dollar industry (McKinlay *et al.*, 2007; Zeikus *et al.*, 1999; Cukalovic & Stevens, 2008; Sauer *et al.*, 2008).

In June 2013, US-based Myriant announced a successful start-up of its flagship bio-succinic acid plant in Lake Providence, Louisiana. This plant is the first of its kind and scale in North America, with a production capacity of 13.6 kt of succinic acid per year, which is expected to increase to 77 kt/a within the next 5 years. Myriant was awarded a US$ 50 million grant by the US Department of Energy towards the construction of this plant, indicating the willingness of government to come on board with a bio-based chemical industry. This comes after the successful start-up of their commercial validation plant in Leuna, Germany, with global partners ThyssenKrupp. It is claimed that their bioprocess reduces greenhouse gas emissions by 93% compared with the equivalent petroleum process (Bastidon, 2012; Hager, 2013). They used a modified strain of *E. coli* in their fermentation process, with several sugars and cellulosic feedstocks as substrate. Myriant also claims that their product will be cost-competitive with petroleum-derived succinic acid down to an oil price of US$ 45 per barrel (Lane, 2012).

Succinity GmbH, a collaborative effort by BASF and Purac subsidiary CSM, aims to produce bio-succinic acid using a BASF-developed bacterial strain, *Basfi succiniproducens*, grown on crude glycerol. The company is currently modifying an

existing fermentation plant near Barcelona, Spain, and is expected to start commercial production in late 2013. This plant will have a capacity of 10 kt/a. Plans to build an additional 50 kt/a facility are also under way (Nuijten, 2012; Bastidon, 2012).

DNP Green and agricultural research and development company ARD have teamed up to form BioAmber, a bio-based chemical company. In 2010, BioAmber commissioned a 2 kt/a bio-succinic acid pilot plant in Pomacle, France, which uses wheat-derived glucose as feedstock, and an engineered *E. coli* strain as biocatalyst. Following this, BioAmber partnered with Mitsui & Co. to build a manufacturing facility in Sarnia, Canada. It will have an initial production capacity of 17 kt/a, which would eventually be increased to 35 kt/a. Commercial production using a genetically modified yeast is expected to start in late 2013. A feasibility study for a 65 kt/a plant in Thailand has already been conducted, and the partners plan to construct a third plant of similar size in either Brazil or North America, resulting in a total cumulative capacity of 165 kt/a (Sheridan, 2011; Bastidon, 2012).

Dutch chemical and biotechnology giant DSM has joined forces with France's Roquette to form Reverdia. A demonstrative bio-succinate plant was built in 2010 in Lestrem, France, and has a production capacity of 0.3 kt/a. Reverdia has adopted a low-pH yeast as their workhorse, which grows under conditions that discourage the dissociation of succinic acid into succinate. This results in easier product purification. The low pH also makes the system less susceptible to infection. Their first commercial plant, based in Cassano, Italy, began construction in 2012, and has an annual capacity of 10 kt. Production is expected to increase to 30 kt/a within the next 5 years (Bastidon, 2012; Chemicals Technology, 2012).

2.3 Succinic Acid Yield Considerations

A proper analysis of the various metabolic pathways must be conducted in order to gain insight into experimentally observed product distributions. Note that the

following discussion ignores biomass formation, so that all theoretical maxima do not consider energy balance closures.

Equation 2.1 describes the maximum stoichiometric yield of succinic acid achievable when 1 mol of glucose is consumed. This relationship translates into 1.12 $g.g^{-1}$ on a mass basis. Equation 2.1 is based on mass and redox balancing.

$$C_6H_{12}O_6 + \frac{6}{7}CO_2 \longrightarrow \frac{12}{7}C_4H_6O_4 + \frac{6}{7}H_2O \qquad \textbf{[2.1]}$$

Most native producers synthesise succinic acid under anaerobic conditions, using a partial tri-carboxylic acid (TCA) cycle. It can be seen from Figure 2.3 that, in these organisms, phosphoenolpyruvate (PEP) is carboxylated to form succinic acid. The path from glucose to succinic acid requires a net consumption of nicotinamide adenine dinucleotide (NADH) and hence is referred to as the reducing branch (red arrows in Figure 2.3). An oxidative branch (blue arrows in Figure 2.3) is therefore required in order balance the cell's redox. Natural producers generate the necessary NADH through the production of acetic acid. Pyruvate may be oxidised via the *pyruvate formate lyase* (PFL) pathway, or the *pyruvate dehydrogenase* (PDH) pathway. The PDH pathway produces NADH, which results in a higher succinic acid yield than that obtained by the utilisation of the PFL pathway. Specifically, a maximum Y_{SS} of 0.87 $g.g^{-1}$ is possible when all pyruvate is fluxed to the PDH pathway, whereas a mere 0.66 $g.g^{-1}$ can be obtained via the PFL pathway. Figure 2.3 gives the redox half-reactions based on the individual oxidative and reductive branches, and the overall reaction used to determine the maximum yields (Van Heerden & Nicol, 2013).

When a full TCA cycle is available, the organism has an additional oxidative pathway at its disposal (Figure 2.4). Both the reducing and oxidative branches of the TCA cycle can therefore generate succinic acid, which would serve to further improve yields. In fact, it can be seen that the resulting overall equation in Figure 2.4 A is the same as Equation 2.1 and therefore the maximum possible yield is achieved. A similar result is obtained when the glyoxylate shunt is employed. Differences in the

relative distribution of carbon between the oxidative and reductive pathways in Figure 2.4 would yield the same overall result (Van Heerden & Nicol, 2013).

Under aerobic conditions, the NADH generated in the oxidative branch of the TCA cycle may be utilised to produce large amounts of adenosine triphosphate (ATP) for growth. This process, known as oxidative phosphorylation, uses oxygen as electron acceptor. The high-energy ATP molecules are used to drive anabolic processes, resulting in rapid growth. Therefore, during aerobic cultivation, biomass production is often favoured over succinic acid synthesis, resulting in a drop in yield (Van Heerden, 2012).

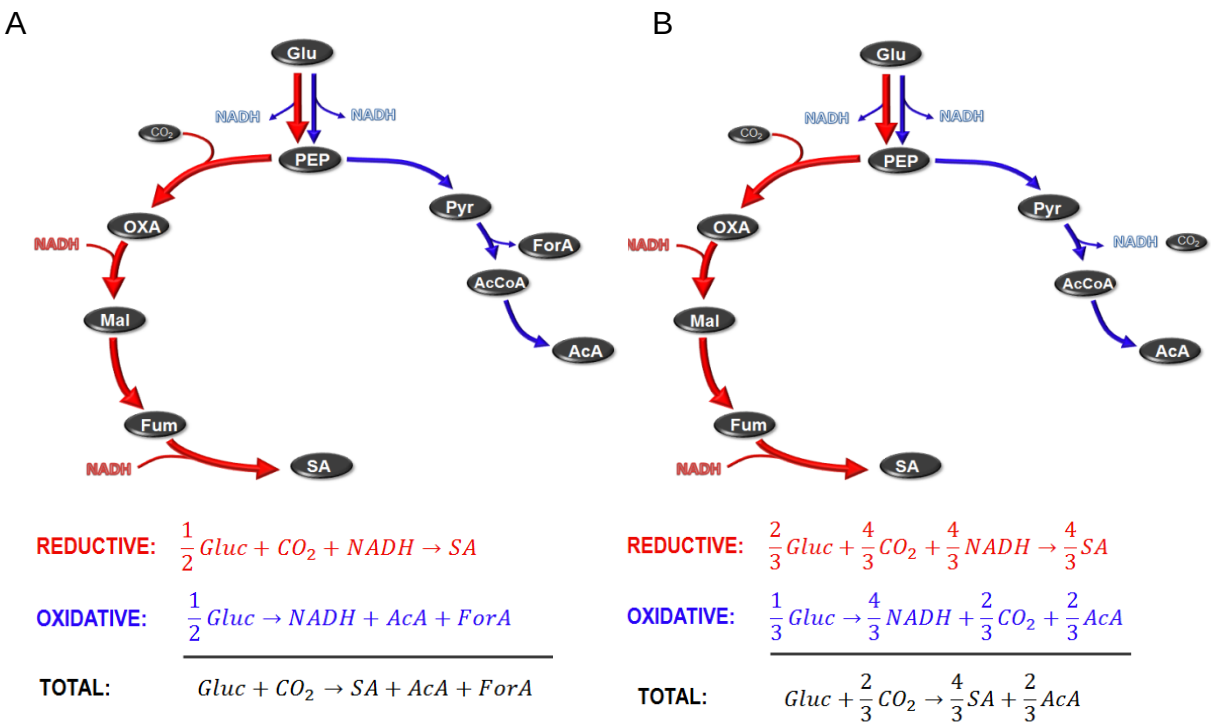

Figure 2.3: *Metabolic pathways of native succinic acid producers. A) Pyruvate oxidation via pyruvate formate lyase, and B) pyruvate oxidation via pyruvate dehydrogenase. Glu – glucose; PEP – phosphoenolpyruvate; OXA – oxaloacetate; Mal – malate; Fum – fumarate; SA – succinate; Pyr – pyruvate; AcCoA – acetyl coenzyme A; AcA – acetate (Van Heerden & Nicol, 2013)*

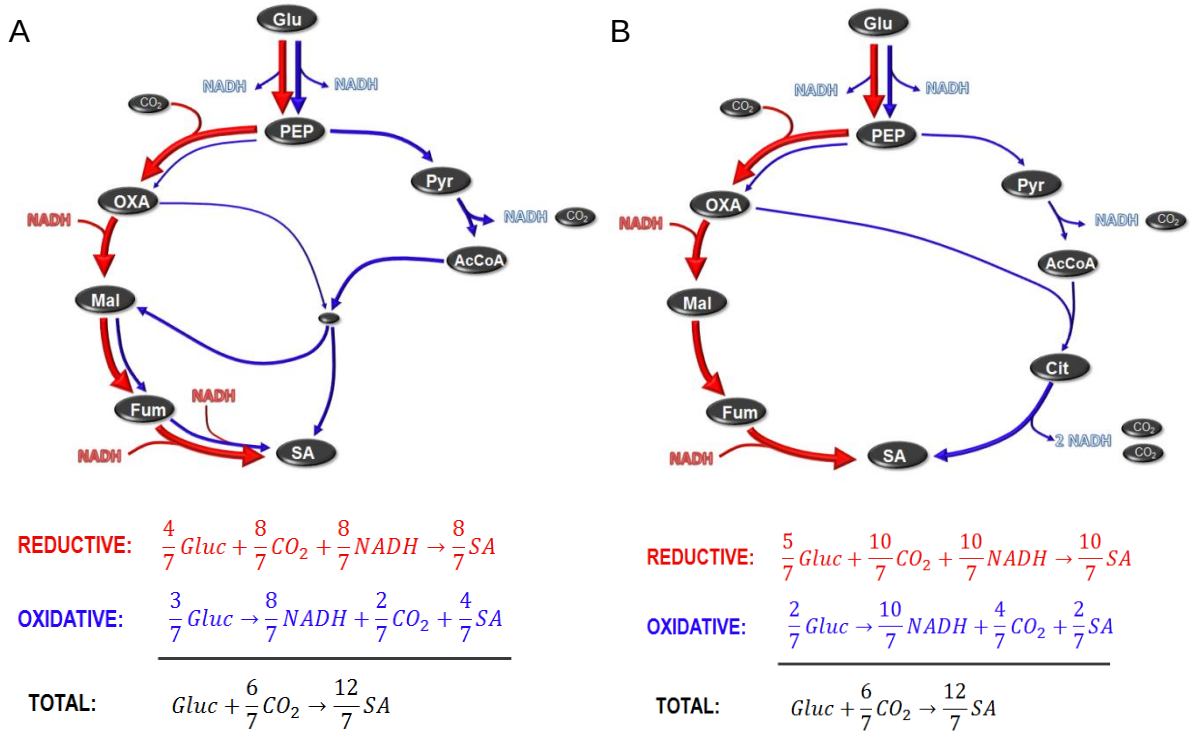

Figure 2.4: *Reductive and oxidative TCA sections, and B) glyoxylate shunt. Glu –glucose; PEP – phosphoenolpyruvate; OXA – oxaloacetate; Mal – malate; Fum – fumarate; SA – succinate; Pyr – pyruvate; AcCoA – acetyl coenzyme A; Cit – citric acid; AcA – acetate (Van Heerden & Nicol, 2013).*

2.4 Biocatalysts

The open literature presents a wide array of organisms with the potential for use in commercial succinic acid production. The most well-studied of these include *Actinobacillus succinogenes*, *Anaerobiospirillum succiniciproducens*, *Mannheimia succiniproducens*, genetically modified *Escherichia coli*, *Enterococcus faecalis*, genetically modified *Yarrowia lipolytica* and *Basfia succiniciproducens* (Van Heerden, 2012; Mwakio, 2012). A few of these are discussed below.

2.4.1 Actinobacillus succinogenes

A. succinogenes, a bacterium from the family *Pasteurellaceae*, is a gram-negative, capnophilic, non-motile, facultative anaerobe. It was first isolated from the rumen of a

cow (Guettler *et al.*, 1996). Four strains have been investigated in the literature, namely 130Z from the American Type Culture Collection (ATCC No. 55618) and three strains from the China General Microbiological Culture Collection Centre (CGMCC): Nos. 1593, 1716 (NJ113) and 2650 (BE-1).To date, no comparison of these strains has been made (Van Heerden, 2012). *A. succinogenes* is unlikely to be pathogenic, which reduces the cost associated with downstream processing, since the reactor effluent does not have to be sterilised.

A. succinogenes lacks certain enzymes required for a full TCA cycle and therefore is unable to achieve the maximum theoretical yield of 1.12 $g.g^{-1}$. It nevertheless produces large quantities of succinic acid, with the major by-products being acetic and formic acids. A simplified metabolic map is provided in Figure 2.5, with values given on a C-mol basis. Ethanol, as well as pyruvic, propionic and lactic acids have also been reported, albeit in minor quantities (Guettler *et al.*, 1996; McKinlay & Vieille, 2008; Li *et al.*, 2010). This bacterium is regarded as a favourable choice for commercial succinic acid production because of its ability to tolerate high acid concentrations. This allows the accumulation of acid in the system, yielding high succinic acid titres and reducing downstream separation costs. Guettler *et al.* (1996) reported achieving 80 $g.L^{-1}$ succinic acid in batch fermentations, while an equivalent fermentation with *A. succiniciproducens* yielded only 37 $g.L^{-1}$.

Another attractive attribute of *A. succinogenes* is its ability to ferment a wide range of substrates. Guettler *et al.* (1996) provide a comprehensive list of carbohydrates that can be utilised by *A. succinogenes*. This list includes some of the most abundant plant-derived sugars, including glucose, fructose, arabinose and xylose. Consequently, various plant-based materials have been investigated for succinic acid fermentation. Among these are corn wastes, cane molasses, cotton stalk, sake lees, wheat and whey (Van Heerden, 2012). The CO_2 required for the fixation reaction may be provided in the form of CO_2 (g), alkaline carbonates and alkaline earth carbonates (McKinlay & Vielle, 2008; Van Heerden, 2012; Mwakio, 2012).

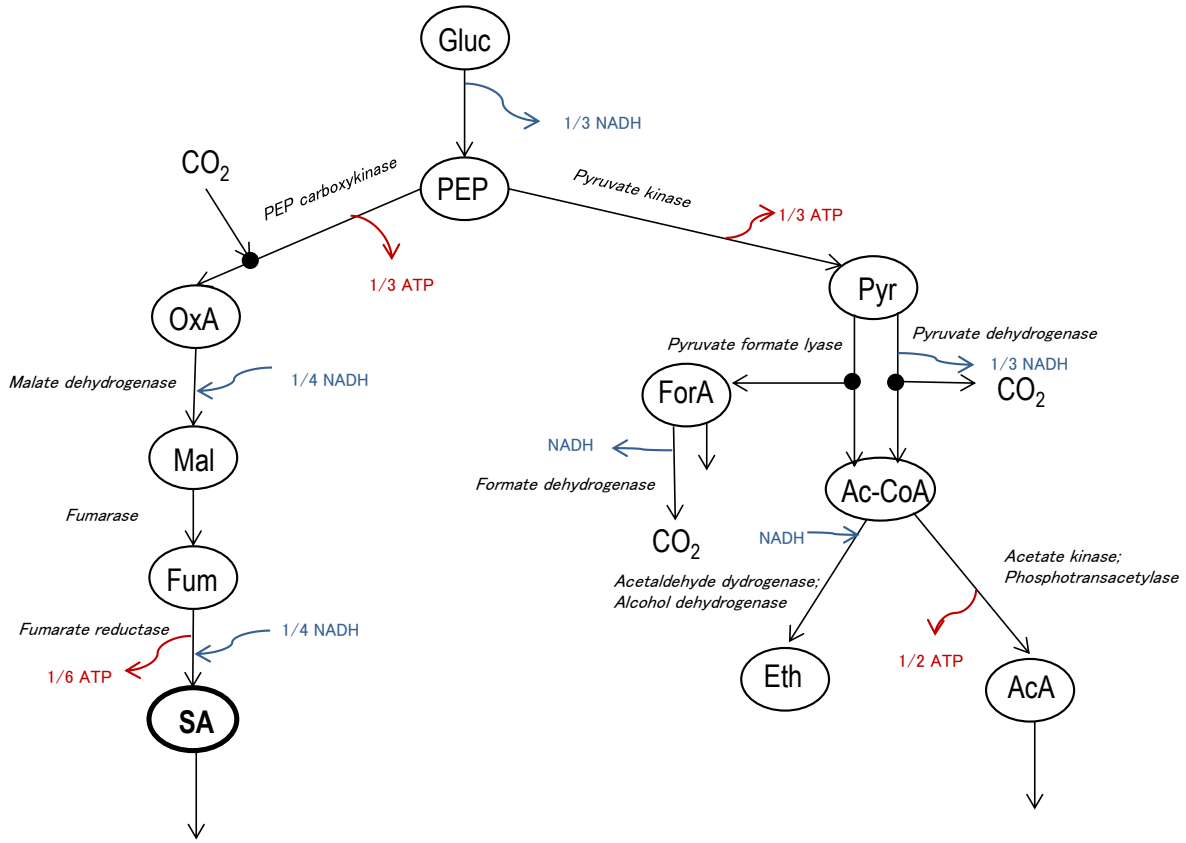

Figure 2.5: *Simplified, C-mol based metabolic map of* Actinobacillus succinogenes *(McKinlay* et al.*, 2010). Gluc – glucose; PEP – phosphoenolpyruvate; OXA – oxaloacetate; Mal – malate; Fum – fumarate; SA – succinate; Pyr – pyruvate; ForA– formate; Ac-CoA – acetyl-coenzyme A; Eth – ethanol; AcA – acetate*

2.4.2 Anaerobiospirullum succiniproducens

A. succiniproducens (ATCC53488), of the family *Succinivibrionaceae*, is a gram-negative, capnophilic, motile, obligate anaerobe. Its inability to grow in the presence of oxygen makes this organism difficult to culture. It has also been reported to have a lower acid tolerance than *A. succinogenes* (Guettler *et al.*, 1996). Like *A. succinogenes*, it produces large quantities of succinic acid, with acetic acid being the major by-product. Small amounts of ethanol, lactic and formic acid have also been reported (Song & Lee, 2006; Samuelov *et al.*, 1991). It is also able to utilise a wide range of substrates, including glucose, fructose, maltose, and glycerol (Van Heerden, 2012). Meynial-Salles *et al.* (2008) obtained the highest glucose-based

succinic acid productivity reported to date (14.8 $g.L^{-1}.h^{-1}$) using a continuous cell recycle reactor. Lee *et al.* (2009), using a single-stage continuous reactor, and Meynial-Salles *et al.* (2008) obtained consistently high yields in excess of 0.75 $g.g^{-1}$. These values are generally higher than the yields reported in continuous *A. succinogenes* studies.

2.4.3 Escherichia coli

E. coli, a member of the family *Enterobacteriaceae*, is a gram-negative, facultative anaerobe. It is one of the most well-researched bacteria, making it a preferred choice for genetic manipulation. Wild strains are able to produce lactate, succinate, acetate and ethanol under anaerobic conditions (Jantama *et al.*, 2008; Sánchez *et al.*, 2005; Vemuri *et al.*, 2002). It has a complete TCA cycle, which allows succinic acid yields to approach the theoretical maximum of 1.12 $g.g^{-1}$. Jantama *et al.* (2008) used a genetically modified strain in anaerobic batch runs, and achieved a Y_{ss} of 1.05 $g.g^{-1}$, a glucose conversion of 69.5%, and a final succinic acid concentration of 73.4 $g.L^{-1}$. *E. coli* can be cultured under aerobic conditions, which encourages rapid growth. This, however, is often associated with a drop in succinic acid yield (Van Heerden, 2012).

2.4.4 Mannheimia succiniproducens

M. succiniproducens (MBEL55E), like *A. succinogenes*, is a member of the *Pasteurellaceae* family, making it a capnophilic, gram-negative, facultative anaerobe. It is metabolically similar to *A. succinogenes*, and produces mainly succinic acid, with acetic and formic acids as major by-products. Lactic acid production under anaerobic conditions has also been reported. In contrast to *A. succinogenes*, it has a complete TCA cycle (Beauprez *et al.*, 2010, Samuelov *et al.*, 1991). It, too, is able to ferment a variety of sugars, including glucose, lactose, fructose, arabitol, mannitol and glycerol (Van Heerden, 2012). A genetically engineered strain, LPK7, eliminates formate and lactate as by-products, with strategies to reduce acetate formation. Acetate, pyruvate and malate were produced alongside 52 $g.L^{-1}$ succinic acid in a fed-batch

fermentation using this strain. A Y_{SS} of 0.76 $g.g^{-1}$ was obtained (Beauprez *et al.*, 2010).

2.5 Bioreaction Studies

The literature available on succinic acid fermentation is vast and varied, and includes studies using different biocatalyst types, substrates, reactor configurations and environmental conditions. The bulk of the available literature concerns batch studies, which is useful for kinetic analyses. However, the kinetics of a particular biocatalyst is usually species-dependent, and research specific to *A. succinogenes* in this regard is limited. The literature available on continuous succinic acid fermentation is usually focused on the overall performance of a given reaction method. Only a handful of studies have dealt with cell immobilisation. A few of the relevant studies are discussed below.

2.5.1 Kinetic parameters

Corona-González *et al.* (2008) used batch fermentations to determine the kinetics of *A. succinogenes* growth and organic acid formation. A clear dissociation of growth- and non-growth-related succinic acid production was observed. This non-growth-related acid production is often the result of *maintenance processes*. Cells require energy for various cell processes. Some of these include the maintenance of various gradients, such as the electro-potential gradient across cell membranes, futile cycles, in which the net result of a given reaction pair is the hydrolysis of ATP, and the turnover of macromolecules, in which large molecules such as RNA are degraded and re-synthesised. All these processes, known as maintenance processes, require energy and therefore substrate is utilised without a net formation of biomass. Such processes must be differentiated from those in which substrate is utilised to form fresh biomass. The following equation, known as the Pirt Equation, can be used to describe the respective contributions made by cell growth and maintenance towards substrate consumption (Villadsen *et al*., 2011: 173):

$$r_s = Y_{xs}^{true}\mu + m_s \quad \textbf{[2.2]}$$

Equation 2.2 suggests that, should growth become negligible, all the consumed substrate would be converted to products for maintenance purposes. In continuous fermentation, the stationary phase of growth is therefore often associated with the highest product yields (Sarika *et al.*, 2012). Y_{xs}^{true} differs from the observed yield in the conversion of substrate to biomass as follows:

$$Y_{sx}^{obs} = \frac{\mu}{Y_{xs}^{true}\mu + m_s} \quad \textbf{[2.3]}$$

Similar expressions can be used for the equivalent product-related parameters (Villadsen *et al.*, 2011: 172–174). It is clear from Equations 2.2 and 2.3 that, in a maintenance-driven system, description of the growth-associated kinetics becomes superfluous.

Corona-González *et al.* (2008) determined that growth stopped when an acid mixture concentration (total succinic, acetic and formic acids) of 22 $g.L^{-1}$, or a succinic acid concentration of 13 $g.L^{-1}$, was obtained. Kim *et al.* (2009), made a similar observation regarding product inhibition, using *A. succinogenes* in continuous fermentations implementing cell recycle. In this case, the exponential growth phase at different dilution rates seemed to end once the succinic acid concentration reached 14 $g.L^{-1}$.

Much higher inhibiting concentrations were obtained in other studies, in which product inhibition was investigated by adding salts of each acid to the growth medium at the start of fermentation. Lin *et al.* (2008), using *A. succinogenes* in batch fermentations, found that growth ceased at a succinic acid concentration of 45.6 $g.L^{-1}$, an acetic acid concentration of 32.3 $g.L^{-1}$ and a formic acid concentration of 10.8 $g.L^{-1}$. In a similar study by Li *et al.* (2010), initial growth inhibition was observed at a succinic acid concentration of 40 $g.L^{-1}$, an acetic acid concentration of 10 $g.L^{-1}$ and a formic acid concentration of 8.8 $g.L^{-1}$. It was suggested (Li *et al.*, 2010)

that the physiology of cells exposed to externally added acids differs from that of cells in which the produced acids are slowly excreted into the medium. Initial addition of the acids allows cells to acclimatise to conditions that inhibit their growth. It is therefore possible that the inhibitory acid titres determined in these studies are actually lower in conventional fermentations. It is interesting to note that, in addition to the findings of Lin *et al.* (2008) and Li *et al.* (2010), several studies cite formic acid as the main growth inhibitor. Ostling and Lindgren (1993) assessed the inhibiting effects of lactic, acetic and formic acids on the growth of 23 strains of enterobacteria. It was found that significant inhibition occurred at formic acid concentrations between 0.005 and 0.07 $g.L^{-1}$, making it the most detrimental product. Similarly, Maiorella *et al.* (1983) found that the most inhibiting product in *Saccharomyces cerevisiae* fermentations was formic acid, with a mere 2.7 $g.L^{-1}$ causing an 80% decrease in cell mass.

The effect of substrate inhibition on growth has also been reported by many authors. Since S_o has a direct impact on S, the initial glucose concentration may be varied to determine the effects of inhibitory substrate titres. Corona-González *et al.* (2008) observed that productivities, conversion yields and specific rates dropped with increasing initial glucose concentration. Substrate inhibition was observed at initial glucose concentrations higher than 30 $g.L^{-1}$, and incomplete conversion obtained at S_o = 85.3 $g.L^{-1}$. Lin *et al.* (2008) also reported a decrease in specific growth rate with increasing initial glucose concentration, with complete growth inhibition observed at S_o = 158 $g.L^{-1}$. Guettler *et al.* (1996) found that *A. succinogenes* could tolerate up to 150 $g.L^{-1}$ dextrose. Mwakio (2012) and Van Heerden (2012) found that doubling the S_o from 20 $g.L^{-1}$ to 40 $g.L^{-1}$ had no significant effect on reactor performance, with similar yields, productivities and titres being achieved at both conditions. The similar acid titres may be attributed to nutrient limitations resulting from the increase in glucose concentration without a corresponding increase in other medium components.

The maximum experimental growth rate observed by Corona-González *et al.* (2008) was 0.41 h^{-1}. This is similar to that achieved in the study by McKinlay and Vieille (2008), in which an experimental μ of between 0.39 h^{-1} and 0.41 h^{-1} was obtained. A

slightly higher experimental μ_{max} of 0.45 h^{-1} was observed by Lin *et al.* (2008), at an initial glucose concentration of 20 $g.L^{-1}$. The maximum experimental growth rate observed by Li *et al.* (2010) was 0.7 h^{-1}, which was obtained when no succinic acid was added to the medium.

The Monod model, amended for substrate and product inhibition, was applied to the data obtained by Corona-González *et al.* (2008). Specifically, the data at S_o = 20.4 $g.L^{-1}$, 32.2 $g.L^{-1}$ and 54.7 $g.L^{-1}$ was used. The following equations for the specific growth rate, specific substrate consumption, and specific succinic acid production were used:

$$\mu = \frac{\mu_{max} S}{\frac{S^2}{K_i} + S + K_s}\left(1 - \frac{C_i}{p_{i,max}}\right) \quad \textbf{[2.4]}$$

$$r_s = Y_{xs}^{true}\mu + M_s \quad \textbf{[2.5]}$$

$$r_p = Y_{xp}^{true}\mu + M_p \quad \textbf{[2.6]}$$

Note that in Equations 2.2 and 2.3 m_s is a constant, while in Equation 2.5 (which is analogous to Equation 2.2), maintenance was made a function of substrate concentration (Villadsen, 2011: 289):

$$M_s = \frac{m_s S}{S + K_{ms}} \quad \textbf{[2.7]}$$

$$M_p = \frac{m_p S}{S + K_{mp}} \quad \textbf{[2.8]}$$

where K_{ms}= 0.51 and K_{ps}= 0.012, determined through optimisation modelling.

True yields were allowed to vary with initial substrate concentration, as it was shown by Lee *et al.* (2009) that Y_{xp}^{true} is dependent on S_o. The fits to the Corona-González

et al. (2008) data can be seen in Appendix 1. The predicted growth-inhibiting succinic acid concentration, p_{max}, is very close to the experimentally determined growth-inhibiting total acid concentration. However, it is higher than the succinic acid-specific inhibiting concentration determined by Corona-González *et al.* (2008). The growth-inhibiting substrate concentration, K_{is}, is only slightly lower than the experimentally determined value of 30 g.L^{-1}.The parameters determined, for the most part, agree quite well with those obtained in the study by Lin *et al.* (2008), in which a similar model was used:

$$\mu = \mu_{\max}(1 - \frac{S}{S_{max}})^n \frac{S}{S+K_s}\left[\prod\left(1 - \frac{c_i}{p_{i,max}}\right)\right] \qquad \textbf{[2.9]}$$

where n=0.603. Lin *et al.* (2008), however, found that true yields seemed to be independent of initial glucose concentration.

Table 2.3 summarises the most important kinetic parameters determined in the above-mentioned studies. Although product inhibition, as mentioned in the literature, may be attributed to all of the produced acids (i.e. succinic, acetic and formic acids), only the succinic acid inhibition parameters are shown.

Table 2.3: *Kinetic parameters reported by various* A. succinogenes *studies*

Reference	S_o ($g.L^{-1}$)	u_{max} (h^{-1})	p_{max} ($g.L^{-1}$)	K_s ($g.L^{-1}$)	K_{is} ($g.L^{-1}$)	Y_{xs}^{true} ($g.g^{-1}$)	Y_{xp}^{true} ($g.g^{-1}$)	m_s ($g.g^{-1}.h^{-1}$)	m_p ($g.g^{-1}.h^{-1}$)
Corona-González *et al.* (2008) *	20.4	0.55	26.6	3.5	30.5	3.4	1.7	0.37	0.2
	32.2	0.55	26.6	3.5	30.5	4	2.3	0.38	0.2
	54.7	0.55	26.6	3.5	30.5	5.6	3.6	0.37	0.2
Lin *et al.* (2008)	0–160	0.5	45.6	2.03	155	4.35	3.6	0.31	0.3
Li *et al.* (2010)	20	0.7	50	-	-	-	-	-	-
McKinlay & Vieille (2008)	9	0.4	-	-	-	-	-	-	-
Guettler *et al.* (1996)	20-150	-	-	-	150	-	-	-	-

*Data obtained in this study was used to determine the parameters in Equations 2.4–2.8

2.5.2 Performance parameters

Table 2.4 summarises the data obtained in the relevant continuous succinic acid fermentation studies. Urbance *et al.* (2004) achieved higher succinic acid concentrations, productivities and glucose conversions using a reduced stirrer speed, where lower shear may have allowed for greater biomass accumulation.

Kim *et al.* (2009) obtained yields and product ratios that appeared to be independent of dilution rate, with SA/AA = 2.5 $g.g^{-1}$, and FA/AA between 0.78 – 0.9 $g.g^{-1}$. A maximum cell concentration of 16.4 $g.L^{-1}$ at D = 0.2 h^{-1} was obtained, which was three times higher than that achieved for an equivalent batch fermentation. A maximum productivity of 6.63 $g.L^{-1}.h^{-1}$ was achieved at D = 0.5 h^{-1}, which was five times higher than that achieved in batch fermentation. Van Heerden (2012) used *A. succinogenes* in several continuous fermentations. Both "chemostat" and immobilised cell reactors were used. In "chemostat" runs, however, biofilm was observed to accumulate gradually on the reactor walls over time, greatly affecting repeatability. Table 2.4 gives the results at possible steady states. A constant SA/AA ratio of about 2.5 $g.g^{-1}$ was achieved in all fermentations, while the acetic acid/formic acid molar ratio approached 1. This is similar to the findings by Kim *et al.* (2009). However, the by-product ratio often dropped below 1 at low dilution rates (D<0.1 h^{-1}). Doubling the initial substrate concentration in "chemostat" runs resulted in the worst succinic acid yields and conversions, with marginal increases in succinic acid concentration. The highest productivities and conversions at a given dilution rate were achieved for the intentional biofilm experiments, using Groperl as supports. The highest productivity obtained was 7.09 $g.L^{-1}.h^{-1}$, during a transient state at a dilution rate of 0.76 h^{-1} (data not shown). It is interesting to note that in the biofilm experiments steady state was achieved much faster than during the "chemostat" runs.

Table 2.4: *Performance parameters of relevant continuous succinic acid production studies*

Authors; Substrate(s)	***D*** (h^{-1})	C_{SA} $(g.L^{-1})$	P_{SA} $(g.L^{-1}.h^{-1})$	Y_{SS} $(g.g^{-1})$	S_o $(g.L^{-1})$	***γ*** $(g.g^{-1})$	***x*** $(g.L^{-1})$
			A. succinogenes				
Kim *et al.* (2009)	0.2	18.6	3.71	0.56	60	0.55	16.4
	0.3	15	4.5	0.55	60	0.46	13.5
S = D-glucose	0.4	15.6	6.25	0.59	60	0.44	13
	0.5	13.3	6.63	0.5	60	0.44	13.1
Urbance *et al.* (2004)	0.2	10.1	2	0.63	20	0.81	N/R
	0.4	9.8	3	0.61	20	0.81	N/R
S = D-glucose	0.6	5.9	3.5	0.51	20	0.58	N/R
	0.8	5.5	4.4	0.53	20	0.52	N/R
125 rpm	1	4.5	4.5	0.4	20	0.56	N/R
(biofilm)	1.2	7.3	8.8	0.46	20	0.8	N/R
150 rpm	0.2	10.4	2.1	0.72	20	0.73	N/R
(biofilm)	0.4	6.2	2.5	0.67	20	0.46	N/R
	0.6	4.8	2.9	0.61	20	0.39	N/R
	0.8	4.6	3.7	0.6	20	0.38	N/R
	1	3.5	3.5	0.48	20	0.37	N/R
	1.2	4.6	5.5	0.61	20	0.38	N/R
Mwakio (2012)	0.04	14.5	0.6	0.72	20	1	N/R
	0.08	14.2	1.1	0.73	20	0.97	2.8
S = D-glucose	0.12	13.9	1.7	0.72	20	0.96	2.35
	0.16	12.5	2	0.73	20	0.86	2.6
	0.2	11.1	2.2	0.7	20	0.79	2.5
	0.24	11.2	2.7	0.62	20	0.90	3.25
	0.28	10.4	2.9	0.6	20	0.86	3
	0.31	10	3.1	0.68	20	0.74	2.6
	0.4	9.9	3.9	0.67	20	0.74	2.2
	0.5	9	4.6	0.64	20	0.7	2
	0.59	8.6	5	0.64	20	0.67	2.2
	0.12	15.6	1.9	0.7	40	0.56	3.6
	0.16	14.8	2.4	0.71	40	0.52	3.2
	0.2	14	2.8	0.66	40	0.53	2

Authors; Substrate(s)	***D***	***C_{SA}***	***P_{SA}***	***Y_{SS}***	***S_o***	***γ***	***x***
	(h^{-1})	***($g.L^{-1}$)***	***($g.L^{-1}.h^{-1}$)***	***($g.g^{-1}$)***	***($g.L^{-1}$)***	***($g.g^{-1}$)***	***($g.L^{-1}$)***
	0.31	10.5	3.3	0.64	40	0.41	2.3
	0.4	9.2	3.7	0.81	40	0.28	2
	0.11	11.5	1.3	0.86	21.5	0.62	N/R
biofilm	0.33	17.0	5.7	0.94	21.5	0.84	N/R
	1.00	11.9	11.9	1	21.5	0.55	N/R
Van Heerden (2012) S = D-glucose	0.04	16.3	0.7	0.64	40	0.64	N/R
	0.14	13.2	1.8	0.58	40	0.57	0.69
	0.32	7.5	2.4	0.56	40	0.34	1.16
	0.085	9.9	0.8	0.66	20	0.75	1.08
	0.12	12.6	1.5	0.65	20	0.96	N/R
	0.15	11.6	1.7	0.66	20	0.88	0.31
	0.17	12.9	2.2	0.71	20	0.91	0.59
	0.21	13.3	2.8	0.67	20	1	1.84
	0.27	7.2	2.0	0.69	20	0.52	0.92
	0.37	9.8	3.6	0.68	20	0.72	1.29
	0.54	9.1	4.9	0.67	20	0.68	N/R
	0.68	5.8	3.9	0.71	20	0.41	0.13
biofilm	0.38	12.5	4.8	0.71	20	0.88	0.93
	0.56	11.1	6.2	0.68	20	0.82	N/R
	0.76	7	5.3	0.73	20	0.48	0.84
			A. succiniproducens				
Meynial-Salles *et al.* (2008) S = D-glucose	0.19	16.2	3.4	0.81	20	1	15.8
	0.23	14.8	3.7	0.74	20	1	18.8
	0.32	16.2	5.5	0.81	20	1	18.6
	0.49	16.2	8.3	0.83	20	0.98	21.3
	0.56	16.5	9.6	0.83	20	0.99	24.5
	0.81	15.9	13.2	0.82	20	0.97	35.6
	0.93	15.5	14.8	0.81	20	0.96	42.4
Lee *et al.* (2009)	0.056	15	0.8	0.79	19	1	0.96
	0.1	14.7	1.5	0.77	19	1	1.06

Authors; Substrate(s)	***D***	***C_{SA}***	***P_{SA}***	***Y_{SS}***	***S_o***	***γ***	***x***
	(h^{-1})	***($g.L^{-1}$)***	***($g.L^{-1}.h^{-1}$)***	***($g.g^{-1}$)***	***($g.L^{-1}$)***	***($g.g^{-1}$)***	***($g.L^{-1}$)***
S = D-glucose	0.18	14.7	2.6	0.77	19	1	1.3
	0.22	14.1	3.1	0.74	19	1	1.35
	0.27	13.7	3.7	0.81	19	0.89	1.45
	0.29	13.1	3.8	0.8	19	0.86	1.42
	0.31	12.2	3.8	0.77	19	0.84	1.49
	0.36	11.7	4.2	0.75	19	0.82	1.47
	0.43	11.3	4.9	0.74	19	0.8	1.47
	0.52	10.2	5.3	0.81	19	0.66	1.49
	0.58	9.7	5.6	0.79	19	0.65	1.45
	0.63	8.3	5.2	0.82	19	0.53	1.27
	0.032	29.6	0.9	0.78	38	0.99	1.38
	0.064	26.5	1.7	0.8	38	0.88	1.6
	0.11	19.5	2.1	0.75	38	0.68	1.32
	0.15	18.5	2.8	0.76	38	0.64	1.29
	0.22	18.1	4	0.75	38	0.63	1.16
	0.41	15.9	6.5	0.73	38	0.57	1.1
	0.54	9.2	5	0.75	38	0.32	0.79
				E. faecalis			
Wee *et al.* (2002) S = fumarate	0.1	30	3	1	30	0.97	N/R
	0.2	28.5	5.7	1	30	0.95	N/R
	0.4	27.3	10.9	1	30	0.95	N/R
	0.1	49	4.9	1	50	0.97	N/R
	0.2	46	9.2	1	50	0.87	N/R
	0.4	37.3	14.9	1	50	0.7	N/R
	0.1	72	7.2	1	80	0.9	N/R
	0.2	55	11	1	80	0.69	N/R
	0.4	42.8	17.1	1	80	0.5	N/R

Mwakio (2012) achieved the highest Y_{SS} and productivity reported in any continuous *A. succinogenes* study to date. Negligible by-product formation resulted in a succinic acid yield approaching 1 $g.g^{-1}$, and a productivity of 11.91 $g.L^{-1}.h^{-1}$, at a dilution rate of 1 h^{-1}. These results were obtained in an immobilised cell reactor, using Groperl as support particles. In "chemostat" runs, however, biofilm was again seen to develop

on the reactor walls. Results and trends similar to those observed by Van Heerden (2012) were reported. However, higher conversions, succinic acid concentrations, yields and productivities were achieved by Mwakio (2012) during immobilised cell runs. It is interesting to note that the suspended cell concentrations reported by Mwakio (2012) are much higher than those achieved by Van Heerden (2012). Furthermore, the formic to acetic acid ratio is much lower in the study by Mwakio (2012). It can be seen from Table 2.4 that a drastic decrease in this ratio is accompanied by a dramatic increase in succinic acid yield. However, an $Mg_2CO_3(OH)_2$ slurry was used to control pH, leading to inaccuracies in dry cell weight measurements, and consequently, poor mass balance closures. The poor mass balances also suggest that the results at D = 1 h^{-1} may be questionable.

Meynial-Salles *et al.* (2008) achieved extremely high succinic acid productivities, yields, conversions and cell concentrations in their two-stage fermentation system. Here, *A. succiniproducens* was used in a bioreactor with an external membrane for cell recycle. A maximum productivity of 14.8 $g.L^{-1}.h^{-1}$ and maximum Y_{SS} of 0.83 $g.g^{-1}$ were achieved. Lee *et al.* (2009), using the same bacterium with no cell recycle, achieved a maximum productivity and succinic acid yield of 6.5 $g.L^{-1}.h^{-1}$ and 0.82 $g.g^{-1}$ respectively.

Wee *et al*. (2002) used a fumarate-reducing bacterium, *Enterococcus faecalis*, immobilised in an inverted hollow-fibre bioreactor (HFBR), for the continuous production of succinic acid. The maximum productivity obtained was 1.7 times higher than that achieved in an equivalent batch run with no cell immobilisation. Although no specific cell concentration data were given, it was reported that the HFBR achieved a cell concentration of approximately 80 $g.L^{-1}$ at all Ds and S_o values. This was about nine times the cell concentration achieved in batch fermentations. From this, it is clear that the HFBR must have been mass transfer-limited, since a significant increase in cell concentration did not translate into a dramatic increase in productivity. This also implies that the cell concentration was not significantly dependent on dilution rate or initial substrate concentration, but rather on the available attachment area.

2.6 Biofilms

2.6.1 Introduction to biofilms

A biofilm is an aggregate of microbial cells enclosed in a matrix. This matrix consists of extracellular products, particulate matter, lysed cell components, ions, polysaccharides, proteins and lipids; up to 97% of the matrix is water (Sutherland, 2001). Extracellular polysaccharides, or EPS, can comprise between approximately 50 and 90% of the total organic matter found in biofilms (Vu *et al.*, 2009). EPS is responsible for the adhesive properties of the biofilm, allowing cells to attach to each other, and to a given surface. The extrapolysaccharides are usually very long, thin chains with a molecular mass of the order of 0.5–2 $\times 10^6$ Da. They are generally heterologous and acidic in nature; in other words, a single polysaccharide would be made up of different monomer types, and usually have a carboxyl, phosphate or sulphate group. These acidic groups have a high affinity for cations such as Ca^{2+}, which offer rigidity to the EPS network. Generally, extracellular polysaccharides are hydrophobic in nature, and tend to interact with the substratum, and other polysaccharides, through hydrophobic interactions (Sutherland, 2001).

Biofilms are normally secreted under conditions of stress, such as nutrient (i.e. nitrogen, phosphates, etc.) limitation. The production of EPS requires the utilisation of extra carbon. As already mentioned, the biofilm matrix has a high water content, which prevents cells from desiccating and allows for the transport of nutrients and communication molecules used in *quorum sensing* (explained below). It also offers protection from shear stresses, anti-microbial agents and phages (Sutherland, 2001). However, the biofilm response may not necessarily be stress-induced. Cells may simply attach to a suitable substrate because of the overall benefits to the colony that the biofilm would provide.

To an individual bacterium, the cost of biofilm formation outweighs the benefits. However, once enough bacteria have accumulated in the system, co-ordinated signals are sent out by neighbouring bacteria, indicating favourable conditions for

biofilm formation. This process is known as quorum sensing (Annenberg Foundation, 2013). Certain genes will then be activated in order to initiate surface attachment. The synthesis of biofilms involves several steps (HyCa Technologies Pvt. Ltd, 2013; University of Glasgow, 2011):

Surface conditioning: Carbohydrates, proteins, ions and other matter attach loosely to the substratum. This forms a conditioning layer on the attachment surface, altering its charge and making it more amenable to biofilm attachment.

Attraction: Weak electrostatic and van der Waals forces attract the bacteria towards the substratum. As the distance between the surface and the cells decreases, stronger, short-range forces, such as hydrophobic interactions, take effect.

Attachment: Bacteria become firmly attached to the surface. Often bacterial appendages, such as pili or fimbrae, are used to keep a firm hold on the surface, while a sticky extracellular polysaccharide is secreted.

Growth and colonisation: The biofilm continues to grow and mature. More free cells are recruited, while cells already present in the biofilm divide. The biofilm comprises a number of diffusion channels which are used for the transport of nutrients and metabolic wastes.

Dispersal: Once the biofilm has reached a critical size, enzymes are secreted in order to detach parts of the biofilm, allowing cells to disperse and colonise other areas.

In order to separate the active, catalytic cells from the biofilm, EPS-cell separations might be attempted. There are various physical and chemical methods available for EPS extraction. Pan *et al.* (2010) compared some of the more common methods found in the literature. Although chemical extractions proved more effective than physical procedures, they were also much more complex. Furthermore, even the best chemical procedures extracted only a small fraction of the total EPS available.

This finding was confirmed by Liu and Fang (2002) – only 165 mg of EPS out of a possible 437 mg were extracted per gram of volatile solids. In addition, EPS determination is subject to interference from complex media components, such as yeast extract (Habibi *et al.*, 2011).

2.6.2 Immobilised cell fermentation

The choice of reactor design in immobilised cell systems is crucial to process efficiency. Batch processes are generally used for low-volume, high-value products, such as pharmaceuticals. Extensive non-productive phases occur between batches, during which the reactor is emptied, cleaned, refilled and sterilised. Therefore, the equipment required to achieve a given production target is often smaller for continuous processes. Continuous operation offers the biocatalyst a relatively constant environment, whereas a batch reactor, by its very nature, contains a medium in which nutrient and product concentrations are constantly changing. The environmental constancy achieved in continuous systems allows better process control. Better efficiency is often obtained within the continuous production chain (Tampion & Tampion, 1987: 184–186). It is for these reasons that a continuous reactor was used in this study.

Immobilised cell reactors can be column, stirred, gas-lift or membrane bioreactors, with fixed, mobile, expanded or fluidised beds. Column reactors with fixed beds are often preferred because of their low cost, ease of scale-up and automation, and generation of low shear forces, consequently avoiding cell damage. This, however, is often associated with low mass and heat transfer rates. Furthermore, the formation of preferential flow channels within the bed reduces reactor efficiency. Solid particles from the medium or dead cell matter may also be trapped in the bed, leading to biocatalyst clogging and deactivation (Baltaru *et al.*, 2009).

Stirred tank reactors offer higher shear rates and therefore better heat and mass transfer rates. Cells may be immobilised on support particles in a bed that is kept mobile by a stirrer, or may attach to the stirrer shaft itself (Urbance *et al.*, 2004).

However, there is also a greater risk of abrasive cell damage. Gas-lift reactors provide a favourable alternative to stirred tank reactors, especially when using filamentous organisms. Fluidised bed reactors may exhibit a range of mixing characteristics. This makes reactor modelling difficult, although good mass and heat transfer rates are usually observed. Membrane reactors can also be used; this includes the use of a membrane for cell recycling, or for direct cell immobilisation within the reactor. However, the biggest problem associated with membrane usage in a cell-recycle system is pore blockage, either by microbial growth on the membrane, or by the flow of biomass and other particulate matter (Tampion & Tampion, 1987: 189, 191, 197, 207 & 209).

Concentration gradients exist between the sites of biocatalytic activity, and the often well-mixed bulk fluid. There are also concentration gradients between the surface of porous support particles and their centres. For example, the concentration of substrate at the liquid-solid interface is lower than in the bulk liquid, and approaches zero near the particle centre (Galaction *et al.*, 2012). This has serious mass-transfer implications. This study looks only at the bulk liquid, and does not consider intra-particle kinetics. Therefore, no attempt to optimise the reactor design for liquid-solid mass transfer was made, and a fixed-bed column reactor was chosen for its simplicity.

The main advantage of cell immobilisation is the increase in cell density in the reactor, resulting in higher volumetric productivities than in free-cell fermentations. Immobilised cells tend to demonstrate a longer life-span than their free-cell counterparts. Free cells often show a decline in activity soon after reaching stationary growth. The stationary phase, however, is often when the formation of economically favourable metabolites is favoured over biomass production. Cell immobilisation tends to extend this phase. Immobilised cells also demonstrate better thermal, chemical, shear force-resistant and growth-inhibition characteristics. Lastly, cell immobilisation allows for easier separation of the biocatalyst from the fermentation medium (Galaction *et al.*, 2012; Flickinger & Drew, 1999: 2667; Sarika *et al.*, 2012). Cell recycling offers an intermediate route between freely suspended and immobilised cell systems, providing high cell densities without the mass transfer

limitations usually associated with immobilised cells (Hatzikioseyian & Remoundaki, *sa*).

Superficial cell adsorption is a very fast and simple immobilisation technique (Fickinger & Drew, 1999: 2667). The surface properties of the cell and substratum (surface charge, surface tension, wettability, composition, porosity and roughness) will determine the strength of the interaction. Self-immobilising cells, such as *A. succinogenes*, are used for cell attachment. Pereira *et al.* (2000) evaluated the potential of several inorganic porous supports for cell adhesion. It was found that foam glass was among those that offered the best support characteristics. Poraver® expanded glass was therefore used for support in this study.

Chapter 3 Experimental

3.1 Culture Strain and Growth

Actinobacillus succinogenes 130Z (DSM 22257 or ATCC 55618) was obtained from the German Collection of Microorganisms and Cell Cultures (Braunschweig, Germany). Stock cultures were cultivated once every two weeks in tryptone soy broth or TSB (Merck KgaA), and incubated in a rotary shaker (100 rpm) at 37 °C for 16–20 h. High-performance liquid chromatography (HPLC) was used to test the culture broth at the end of the incubation period for lactic acid contaminants. Stock cultures were then stored at 5 °C.

3.2 Medium

The medium composition, given in Table 3.1, was based on a formulation by Urbance *et al.* (2003). This medium was used in three continuous, immobilised *A. succinogenes* studies, viz. Urbance *et al.* (2004), Mwakio (2012) and Van Heerden (2012). However, in this study, $Na_2S.H_2O$ was excluded in an attempt to simplify the medium, with no observable effects on reactor performance. The initial glucose concentration used by Urbance *et al.* (2004) was 20 $g.L^{-1}$, while Van Heerden (2012) and Mwakio (2012) both used 20 $g.L^{-1}$ and 40 $g.L^{-1}$. In this study, glucose was added to the medium at approximately 35 $g.L^{-1}$ for dilution rates of about 0.3 h^{-1} to 0.7 h^{-1}, but increased to about 60 $g.L^{-1}$ at low dilution rates (D = 0.11 h^{-1} & 0.054 h^{-1}) in order to avoid substrate limitation. Antifoam was added at a much higher concentration than that used by Van Heerden (2012), i.e. 1 $mL.L^{-1}$. However, no drop in reactor performance was observed and the problem of foaming in the reactor was effectively reduced, thereby allowing good control of the liquid level.

Table 3.1: *Final medium composition*

Compound	***C_i (g.L^{-1})****	***Source***
Corn steep liquor	10.00	Sigma-Aldrich
Yeast extract	6.00	Merck KgaA
Antifoam A*	1.00	Sigma-Aldrich
$CaCl_2.H_2O$	0.20	Merck KgaA
K_2HPO_4	3.00	Merck KgaA
$MgCl_2.6H_2O$	0.20	Merck KgaA
NaCl	1.00	Merck KgaA
Na_2HPO_4	0.31	Merck KgaA
NaH_2PO_4	1.60	Merck KgaA
NaOAc	1.36	Merck KgaA
D-glucose	35 or 60	Merck KgaA

*C_i given in mL.L^{-1}

The corn steep liquor was first mixed with distilled water to a concentration of 200 g.L^{-1} and boiled (5 min, 105 °C) to remove components that would otherwise precipitate out after autoclaving the medium (Sikyta, 1995: 153). After the precipitate had settled, the required volume of clarified corn steep liquor solution was added to the medium. It was assumed that the concentration of the clarified liquor remained at 200 g.L^{-1}.

The phosphates (K_2HPO_4, Na_2HPO_4 and NaH_2PO_4) and glucose were sterilised separately and then added to the medium once the feed bottle had cooled. This avoided the formation of complexes that may have affected usable protein and carbohydrate concentrations in the medium (Plank, 2012).

3.3 Apparatus

The reactor is shown in Figure 3.1, with a few basic dimensions provided. It consisted of an aluminium base and head, separated by a glass column. O-rings sealed off the head and base from the atmosphere. All reactor ports were ¼ ” stainless steel tubes.

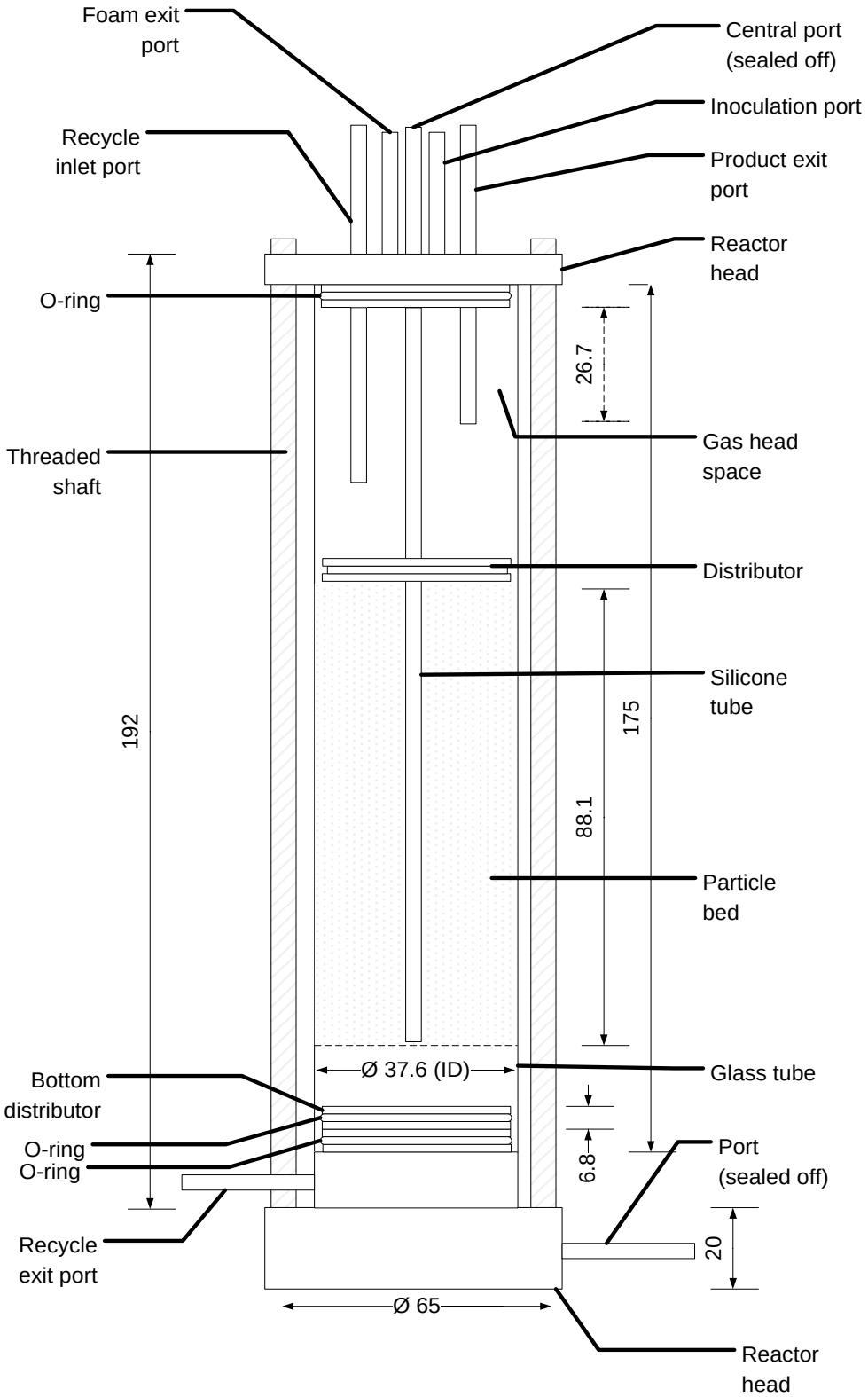

Figure 3.1: *Bioreactor used in experimental set-up*

Upon the head were five ports: an inoculation, recycle inlet, product exit and foam exit port, while the extra port was sealed off from the atmosphere. The extra port was used to attach a piece of silicon tubing to the reactor head, which extended into the reactor. This tubing was threaded through a central hole in a distributor and held the distributor in place. The distributor, in turn, acted like a sieve and kept the support particles fixed. The diameter of the distributor holes (3 mm, triangular pitch) was chosen so as to prevent the support particles from washing out, while allowing gas and liquid to flow through easily, thereby preventing the formation of concentration gradients above and below the distributor. The recycle inlet was just above the distributor. The product exit port was situated just above the recycle inlet. The inoculation port had a short piece of silicon tubing attached to it and was sealed off from the atmosphere by a silicon stopper. The base of the reactor had a distributor with holes 1 mm in diameter, which allowed for good gas-liquid distribution. According to Suja and Donnelly (2006), a liquid-filled space between the reactor floor and particle bed promotes good gas-liquid mixing, as the gas bubbles hit the bed with greater impact. Therefore, there was always about a centimetre of reactor length between the bottom distributor and the base of the particle bed. An extra O-ring around the bottom distributor allowed for further sealing near the base of the reactor. Below the bottom distributor were two ports: the first served as the recycle exit into the reactor, while the second was sealed off from inside the reactor and remained unused.

The total working volume of the reactor was 165 mL. *A. succinogenes* was immobilised on Poraver® (Dennert Poraver GmbH) expanded glass particles with 3 mm < d_p ≤ 4 mm and a bulk density of 190 ± 20 kg.m^{-3} (Dennert Poraver GmbH, 2013). Poraver® is a cheap, recyclable, pressure-resistant material. The support particles occupied a volume of ± 65 mL (about 39% of the working volume). Before each run, a constant mass of dry support particles was measured out (15.73 g), thereby ensuring a more or less constant volume of Poraver® in the reactor. It also ensured a more or less constant surface area available for attachment in each run.

The reactor set-up can be seen in Figure 3.2 and Table 3.2 details the components. A pump on the exit line was used to control the liquid level inside the reactor. This

allowed a gas head to be established inside the reactor. A foam trap bottle allowed any gas build-up in the reactor to be released to the atmosphere. If foam were to develop and fill the gas head space, it would flow into the foam trap, where mechanical stirring would break up the foam, releasing the gas into the atmosphere.

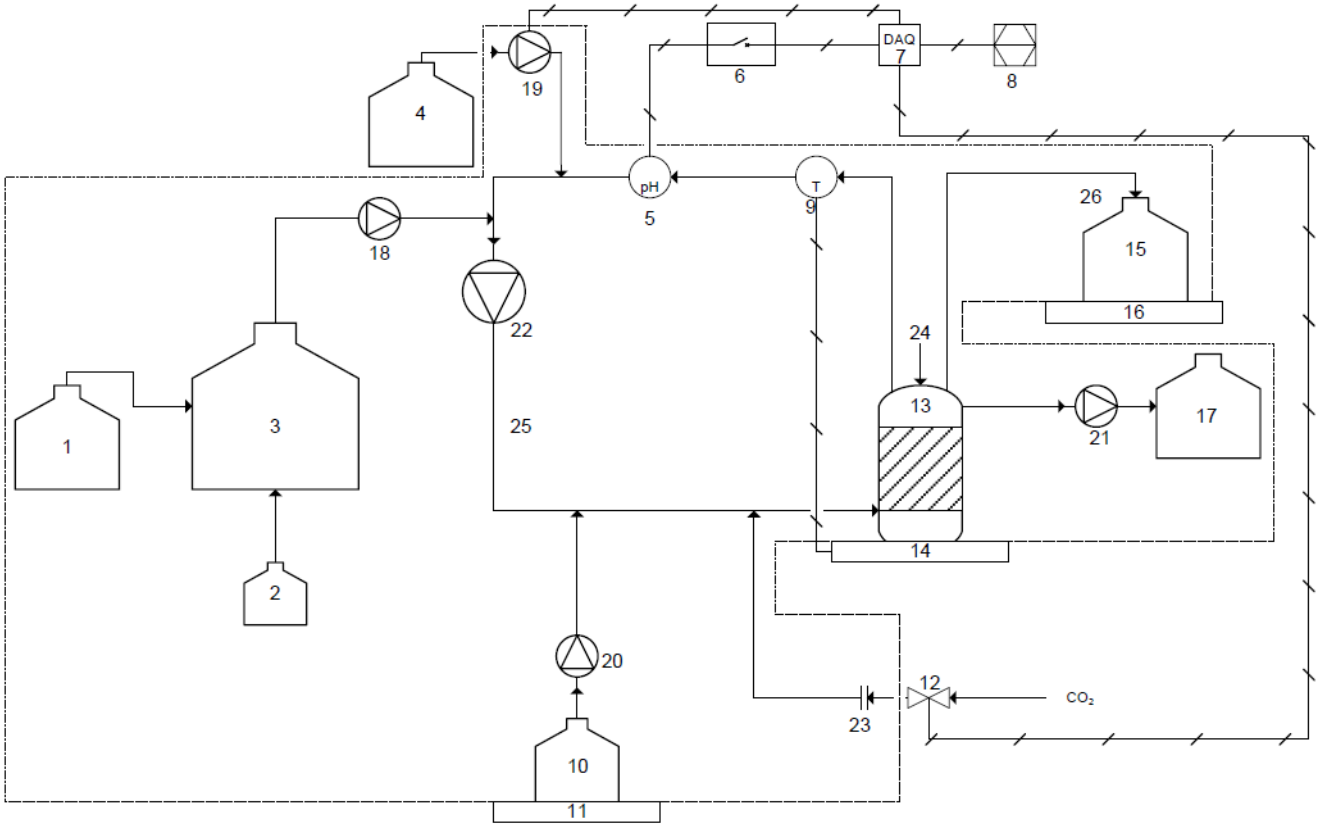

Figure 3.2: *Continuous fermentation set-up using immobilised* A. succinogenes. *Dotted lines indicate those components that were connected and autoclaved before each fermentation*

Table 3.2: *Equipment used in experimental set-up (see Figure 3.2)*

No.	*Equipment description*	*Details*
1	Glucose	-
2	Phosphates	-
3	Feed reservoir	-
4	Base reservoir	-
5	pH probe	Endress & Hauser Tophit CPS471
6	pH controller	Endress & Hauser Liquiline CM442
7	Data acquisition (DAQ)	National Instruments – NI USB-6008
8	Personal computer	-
9	Thermocouple	Integrated in hot plate (see No. 14)
10	Antifoam reservoir	-
11,14,16	Hot plate/Stirrer	Heidolph Instruments – MR Hei-Standard
12	Control valve	Brooks 5850E Mass Flow Controller
13	Bioreactor	Custom made
15	Foam trap	-
17	Product reservoir	-
18,19,20,21	Peristaltic pump	Watson-Marlow 120U
22	Peristaltic pump	Watson-Marlow 323
23	0.2 µm filter	Sartorius – Midistart 2000
24	Inoculation port	-
25	Recycle line	-
26	Sample line	-

Temperature and pH were controlled at 37 ± 1 °C and 6.8 ± 0.05 respectively. Below the reactor was a hot plate, used for temperature control, and an aluminium thermowell in the recycle line housed the thermocouple. An autoclavable pH probe in the recycle line was connected to a controller, which intermittently activated a pump that dosed a solution of unsterile 10 M NaOH into the reactor as required.

3.4 Fermentation

The entire reactor set-up (excluding the 10 M NaOH solution – see dotted lines, Figure 3.2) was connected and autoclaved at 121 °C. For a 5 L feed bottle, autoclaving time was 40 min, but this was increased to 60 min for a 10 L feed. All bottles were fitted with 0.2 µm PTFE (polytetrafluoroethylene) gas filters, to allow air, steam and CO_2 (g) to enter and exit the bottles as necessary.

Using a larger feed bottle meant fewer feed changes, and hence fewer opportunities for infection to be introduced. Feed changes were carried out by first preparing and autoclaving fresh medium, glucose and phosphates. Once cooled, the individual components were mixed, and the new medium was pumped into the old feed bottle via a stainless steel connection. This connection was sterilised in a 140 °C oil bath for 20 min just prior to transfer.

The line connecting the fermentation system to the 10 M NaOH bottle remained clamped until just before it was immersed in the base reservoir. It was assumed that any contaminating bacteria entering the line during this brief moment would be killed by the highly basic solution.

Inoculum was prepared similarly to stock cultures (see Section 3.1 Culture Strain and Growth). Stock cultures (6.7 %v/v) were used to inoculate the TSB-filled vials to be used as inoculum for the fermentation. This was done about 16–20 h before inoculation of the reactor was to take place. A sterile syringe/needle configuration was used to transfer the inoculum from the vial into the reactor, by piercing the silicone stopper in the inoculation port. The needle was kept in a flame while transporting the inoculum-filled syringe from the laminar flow hood to the reactor, and the top surface of the silicone stopper was dosed with 70% ethanol before inserting the needle. The needle/syringe configuration was kept in the stopper throughout the fermentation. About 4 mL of inoculum (24 %v/v) was used each time. Before inoculation, the reactor was run in batch mode for about 12–16 h in order to ensure sterility of the reactor set-up. Temperature and pH control were initiated prior to inoculation. After inoculation, the reactor was run in batch mode for about 12–16 h. The feed flow rate was then adjusted to give the required D.

At low dilution rates (high succinic acid concentrations), a mixture of propylene glycol and Antifoam A was dosed into the recycle on an as-needed basis. Six parts of propylene glycol were added to one part Antifoam A (Sigma-Aldrich, 2013). CO_2 (7% vvm) was continuously sparged into the reactor, since the production of 1 mol succinic acid requires the fixation of 1 mol CO_2. It was shown in earlier experiments

(data not shown) that increasing the CO_2 concentration from 5 % vvm to 10 % vvm had negligible effects on both productivity and product distributions. It was therefore assumed that under these conditions, the fermentation broth remained CO_2-saturated at all times, i.e., gas-to-liquid mass transfer was not rate limiting. CO_2 (g) was passed through a 0.2 µm PTFE gas filter before entering the recycle line downstream of the recycle pump. The recycle flow rate was kept constant at 140 rpm (497 mL.min^{-1}) in all fermentations in order to maintain similar shear conditions.

For dilution rates ≥ 0.31 h^{-1}, biofilm formation would occur after ± 2 days. At lower dilution rates, no biofilm growth was observed even after 3 days. This may have been due to the slow growth usually associated with the high inhibitory acid titres observed at low Ds. Therefore, to test the biofilm reactor performance at lower dilution rates, the reactor was first operated at a high D (D ≥ 0.3 h^{-1}) in order to rapidly establish a biofilm. Once the system had more or less reached a steady state, the feed flow was dropped to give the required lower D. At the higher Ds, a glucose concentration of ± 35 g.L^{-1} was used to avoid any potential substrate inhibition. Once the D had been lowered, the initial glucose concentration was increased to about 60 g.L^{-1} in order to avoid substrate limitation.

A wide range of operating dilution rates were chosen (D = 0.054 h^{-1} – 0.72 h^{-1}) in order to assess system kinetics and process performance under greatly varying conditions. Dilution rates of approximately 0.1 h^{-1}, 0.3 h^{-1} and 0.7 h^{-1} were used to assess system repeatability. In Run 7, S_o was increased from ± 35 g.L^{-1} to ± 60 g.L^{-1} at D = 0.31 h^{-1} in order to observe the effects, if any, of substrate inhibition. Further details on the choice of reactor conditions can be found in Table 4.1.

3.5 Analysis

Product samples were collected from the reactor exit line as required. Organic acid and substrate concentrations were determined by high performance liquid chromatography (HPLC). An Agilent 1260 Infinity HPLC (Agilent Technologies, USA), equipped with a 300 x 7.8 mm Aminex HPX-87H column (Bio-Rad

Laboratories, USA) and a refractive index detector (RID) was used. The mobile phase used was 5.6 mM sulphuric acid at a flow rate of 0.6 ml.min^{-1}. The column temperature was 60 °C. Succinic and acetic acids detected in the medium were subtracted from their corresponding outlet concentrations, as determined by HPLC analysis.

Stock culture, inoculum, medium and product samples intended for HPLC analysis were first centrifuged at 13 400 rpm for 90 s. The supernatant was then passed through a 0.45 µm nylon filter, attached to a syringe.

Once the reactor had reached a steady state, a large-volume product sample was collected over a period of 12–24 hours, depending on the D. Shorter time periods were used for higher dilution rates. The product bottle was kept in ice for the duration of the collection period in order to prevent further growth and metabolism. The collected volume was then thoroughly mixed, and a 100 mL sample collected for suspended cell analysis. This was performed by splitting the 100 mL sample into 10 x 10 mL samples, and centrifuging at 4 000 rpm for 10 min. The samples were centrifuged three times. After each centrifugation, the supernatant was decanted, and the cell pellets washed in distilled water. Following the third centrifugation, the cell pellets were transferred to a pre-measured vial. These were then dried to a constant weight in an 85 °C oven.

Total biomass quantifications (TBQs) were also required once steady state had been reached. This involved determining the dry cell weight of all biomass present in the reactor, including suspended cells and attached biofilm. This was obtained by first stopping the feed flow and running the reactor in batch mode. The recycle flow rate was increased to 200 rpm (703 mL.min^{-1}). The recycle line was then opened and the entire liquid content of the reactor pumped out into a 2 L collection bottle. The reactor was then refilled with distilled water and the wash-out process repeated. After washing with distilled water for a second time, the reactor was dismantled and the Poraver® carefully emptied into a pre-measured glass beaker. Residual biofilm observed inside the reactor was scrubbed clean using distilled water and added to

the collection bottle. The volume of the collection bottle was then topped up to 2 L. A sample size of 200 mL (10%, volume basis) was taken from the collection volume to be analysed for dry cell weight. The sample was split into 20 x 10 mL samples and centrifuged for 10 min at 4 000 rpm. After each centrifugation, the supernatant was removed and the cell pellets washed in distilled water. Following the third centrifugation, the cell pellets were transferred to a pre-measured vial. The cell pellets and Poraver® were then dried to a constant weight in an 85 °C oven. A basic calculation gave the total biomass concentration in the bioreactor on a dry weight basis:

$$X_{tot} = \frac{A_a - A_b}{V} + \frac{DCW_{vial}}{0.2} \times \frac{V_{collection\ bottle}}{V} \quad \textbf{[3.1]}$$

where A_a and A_b are the Poraver® masses after and before the experiment respectively.

LabVIEW SignalExpress (National Instruments) was used to control CO_2 flow rate, record pH and time-averaged base dosing. Time-averaged base dosing calculated the average flow rate of the NaOH solution pumped to the reactor in order to neutralise the produced acids and maintain the pH.

Steady state was assumed when either:

I. The absolute average deviation of the NaOH molar flow rate, captured over a period of at least 12 h, did not exceed 10% of the mean value, or

II. The absolute maximum deviation of a set of succinic acid data, captured over a period of at least 12 h, did not exceed 10% of the mean value.

The absolute average deviation was used for the NaOH flow data because of the noise associated with the time-averaged signal and the vast amount of data available (data were captured every second). The absolute average deviation would therefore give a good representation of the system during the time period in

question. The absolute maximum deviation was used for succinic acid experimental data because only a few data points were captured at any given steady state. In this case, an absolute average deviation would only serve to dampen the effects of outliers. In most cases, these two criteria correlated. In some situations, only the first criterion was used to determine steady state. In these situations, time constraints dictated that the final HPLC sample ordinarily taken in order to confirm the second criterion could not be obtained.

Volume balancing was based on the assumption that the density of the reactor contents remained constant. Volume balances were performed in order to ensure that an accurate effective D was used in calculations. This calculation compared the actual volumetric reactor throughput with the expected volumetric flow. The actual volumetric flow was based on the volume collected in the product bottle in a given time. The expected volumetric flow was calculated by adding the feed, NaOH and antifoam flow rates (where applicable) based on pump calibrations. The following equation was used:

$$\%\, Volume\ accounted\ for = \frac{V^{actual} - V^{calculated}}{V^{actual}} \times 100 \qquad \textbf{[3.2]}$$

The largest errors (> 5%) in the volume balance occurred at high succinic acid titres, when the system was prone to foaming. In these cases, $V^{calculated}$ was used to determine an effective D since pump calibrations were seen to remain accurate throughout the study. The effective D based on $V^{calculated}$ was then checked against a mass balance (see below). If the mass balance closed to within 5%, it was assumed that the calculated volumetric flow gave an accurate representation of the system. If not, the HPLC data from the sample in question were checked against previous data at a similar condition for consistency. If the data proved consistent, the sample was considered valid.

In Run 1, foaming caused volume balance errors exceeding 10%. However, according to the criteria discussed above, all data obtained during this run proved to be valid. In later runs, an anti-foam bottle was kept on-line in order to control the

foaming when necessary. Early on in Run 2, volume balances again exceeded 10%. This was because anti-foam dosing was initiated only once biofilm was observed to develop, since it had been seen to otherwise inhibit the initial attachment phase. Again, the data were considered valid, despite the volume balance errors. These errors fell to below 5% once anti-foam dosing was initiated. Table 3.3 presents the average volume balance closures obtained in Runs 3–7 at the relevant dilution rates. The scatter in these values has been captured by the absolute average deviation (AAD). Further details on volume balances can be found in Appendix 2.

Table 3.3: *Average volume balance closures*

	***D* (h^{-1})**	***% Volume accounted for*[1]**	***AAD (%)*[2]**
Run 3	0.70	103.6	1.3
Run 4	0.72	101.9	0.2
	0.11	94.1	1.0
Run 5	0.31	100.3	2.1
	0.11	103.6	0.0
Run 6	0.52	100.8	1.5
Run 7	0.32	99.0	0.7
	0.31	99.0	0.7
	0.11	104.3	1.2
	0.05	104.9	3.4
	0.72	94.9	0.2

[1] Each value is an average of all volume balances (one for every sample taken) performed during the described run and corresponding D. It therefore gives a representation of data captured at steady and pseudo-steady states.

[2] The average volume balance figure ("% Volume accounted for") was subtracted from each of the data points used in obtaining this average and an absolute difference obtained. These absolute differences were then averaged among the number of data points used in calculating the corresponding average.

Mass balances required the experimental concentrations of the produced acids, as well as the glucose outlet concentrations. Suspended cell values obtained by Van Heerden (2012) and Mwakio (2012) indicated that the carbon flux to biomass is negligible. Therefore, for the purposes of simplification, mass balance calculations

neglected biomass formation and consequently, excluded a nitrogen source. Small suspended cell values and good mass balance closures (Table 3.4) later proved this assumption to be valid for this study. The expected $S_{o,adj}$ value was calculated and compared with the actual $S_{o,\,adj}$ value:

$$\%\, Mass\ accounted\ for = \frac{{S_{o,adj}}^{actual} - {S_{o,adj}}^{calculated}}{{S_{o,adj}}^{actual}} \times 100 \qquad \textbf{[3.3]}$$

The actual $S_{o,adj}$ value was determined by first performing an HPLC analysis on a single sample obtained from the medium bottle. This value (S_o) was then adjusted according to the total flow rate into the reactor, i.e. the effective D. The total flow rate included the feed flow, the average NaOH flow and the antifoam flow, where applicable. Equation 3.4 was used to calculate the stoichiometries of the respective components, and, consequently, ${S_{o,adj}}^{calculated}$:

$$\boldsymbol{A}\ Gluc + \boldsymbol{B}\ CO_2 \longrightarrow \boldsymbol{C}\ SA + \boldsymbol{D}\ AcA + \boldsymbol{E}\ ForA + \boldsymbol{F}\ H_2O \qquad \textbf{[3.4]}$$

where A–F are the unknown stoichiometries. These were then calculated using C-, H- and O-elemental balances, and the experimental inputs.

Mass balance closures within an absolute error of 5% were considered acceptable. If this criterion was not met, the data were checked against previous data at a similar condition for consistency, before it was decided whether they should be disregarded. Table 3.4 gives the average mass balance closures obtained in each run at the relevant dilution rates. The scatter in these values has been captured by the AAD. Further details on mass balances can be found in Appendix 2. It can be seen that the mass balances usually met the 5% acceptability criterion. Generally, mass balances that did not meet this criterion correlated with low Ds (≤ 0.11 h^{-1}) or unstable growth periods at D ≥ 0.7 h^{-1} (Appendix 2).

Table 3.4: *Average mass balance closures*

	D (h^{-1})	*% Mass accounted for*[1]	*AAD (%)*[2]
Run 1	0.32	99.5	2.3
Run 2	0.32	99.5	3.4
Run 3	0.70	101.6	5.3
Run 4	0.72	97.6	0.7
	0.11	90.4	1.8
Run 5	0.31	100.6	1.4
	0.11	91.6	0.7
Run 6	0.52	100.8	1.5
Run 7	0.32	105.2	2.1
	0.31	91.7	2.0
	0.11	93.6	1.0
	0.05	93.9	0.7
	0.72	94.5	1.2

[1] Each value is an average of all mass balances (one for every sample taken) performed during the described run and corresponding D. It therefore gives a representation of data captured at steady and pseudo-steady states.

[2] The average mass balance figure ("% Mass accounted for") was subtracted from each of the data points used in obtaining this average and an absolute difference obtained. These absolute differences were then averaged among the number of data points used in calculating the corresponding average.

Volume and mass balances performed on "transient" data (i.e. data that did not fulfil the steady state criteria described above) suggest that accumulation, which is zero for a system at steady state, is small. Although there is a slow accumulation of cells over time, the rate of this accumulation is much slower than the overall system kinetics. It can therefore be concluded that "transient" conditions in this study actually corresponded to a system pseudo-steady state. In this text, "steady state" will refer only to data that fulfil the two criteria discussed above.

Chapter 4 Results and Discussion

4.1 Main Results

The reactor conditions maintained in each run are given in Table 4.1. The duration for which the reactor was operated under the described conditions, as well as the reasons for the choice in variables, namely D and S_o, are also provided. Note that the S_o values quoted in Table 4.1 are approximate values; more accurate values can be found in Table 4.2 and Appendix 2. As already mentioned in Chapter 3, the lower S_o value of approximately 35 $g.L^{-1}$ was generally used for $D \geq 0.3$ h^{-1}. This was done in order to mitigate any possible substrate inhibition and to encourage rapid biofilm growth. For lower dilution rates, the higher S_o of approximately 60 $g.L^{-1}$ was used to prevent substrate limitation. Total steady state biomass quantifications were essential for evaluating the system kinetics. The various dilution rates were also used to assess the process parameters under widely varying conditions.

Table 4.1: *Independent reactor variables, reasons for chosen variables and duration of experiment*

	D (h^{-1})	S_o ($g.L^{-1}$)	Duration (d)	Primary objective(s) of run
Run 1	0.32	35	3.9	Total steady state biomass quantification for kinetic analysis
Run 2	0.34	35	4.7	Repeatability check
Run 3	0.70	35	2.0	Total steady state biomass quantification for kinetic analysis
Run 4	0.72 0.11	35 60	1.6 1.9	Total steady state biomass quantification for kinetic analysis; Repeatability check
Run 5	0.31 0.11	35 60	3.2 1.4	Assess path-dependency of steady state conditions (repeatability)
Run 6	0.53	35	3.1	Total steady state biomass quantification for kinetic analysis
Run 7	0.31 0.31 0.12 0.05 0.72	35 60 60 60 35	6.0 4.0 5.5 4.4 2.5	Stability check at D = 0.31, 0.12, 0.054 & 0.72 h^{-1}; Determine effects of S_o

Table 4.2 provides a summary of the steady state data obtained in this study. Further details on individual runs can be found in Appendix 2. Note that total biomass quantifications could only be performed at the end of a run.

There is significant scatter in the suspended cell data, despite the fact that 12–24 h samples were collected and analysed. The erratic nature of biofilm sloughing could account for this scatter. Generally, high yields were observed. The highest steady state Y_{SS} value was 0.89 $g.g^{-1}$, obtained when D = 0.31 h^{-1} (Run 7). The highest productivity obtained was 10.7 $g.L^{-1}.h^{-1}$ at D = 0.7 h^{-1} (Run 3), and the succinic acid titre reached 36.4 $g.L^{-1}$ at D = 0.054 h^{-1}.

Table 4.2: *Summary of steady state results*

	D (h^{-1})	S_o ($g.L^{-1}$)	$S_{o,adj}$[1] ($g.L^{-1}$)	S ($g.L^{-1}$)	SA ($g.L^{-1}$)	AcA ($g.L^{-1}$)	$ForA$ ($g.L^{-1}$)	X_{tot} ($g.L^{-1}$)	X ($g.L^{-1}$)	P_{SA} ($g.L^{-1}.h^{-1}$)	Y_{SS}[2] ($g.g^{-1}$)
Run 1	0.32	36.5	33.7	7.2	22.6	5.6	1.6	23.7	-	7.3	0.85
Run 2	0.34	36.6	34.1	8.1	20.7	5.1	2.5	-	-	7.0	0.79
Run 3	0.70	36.7	34.8	13.7	15.3	4.8	2.5	22.4	-	*10.7*	0.72
Run 4	0.72	37.2	35.7	19.1	12.0	3.9	2.7	-	-	8.6	0.72
	0.11	61.5	57.2	18.3	29.2	5.3	0.3	27.9	0.22	3.3	0.75
Run 5	0.31	37.2	35.0	11.2	20.2	5.6	2.3	-	-	6.3	0.85
	0.11	58.1	53.7	16.4	30.3	5.9	0.8	-	0.64	3.4	0.81
Run 6	0.53	36.6	33.7	16.8	13.5	4.5	2.3	21.2	1.20	7.1	0.80
Run 7	0.31	34.9	33.2	7.5	22.8	5.8	1.7	-	-	7.0	*0.89*
	0.31	60.4	57.2	31.6	18.9	5.0	1.7	-	0.79	5.8	0.74
	0.12	60.4	54.4	20.9	28.3	6.6	1.1	-	1.75	3.2	0.84
	0.05	60.4	52.0	10.1	*36.4*	8.3	0.4	-	2.50	2.0	0.87
	0.05	60.4	52.2	15.5	32.2	7.9	1.1	-	2.80	1.7	0.88
	0.72[3]	34.1	32.7	17.1	11.4	4.2	3.2	-	-	8.2	0.73

Highest yield, productivity and succinic acid titre have been italicised.

[1] The effective glucose concentration entering the reactor based on the total flow

[2] Based on $S_{o,adj}$

[3] Although a steady state, as described in Section 3.5, was not obtained at this condition, the dosing profile plateaued for a period of about 6 h (> 4 volume turnovers). Therefore the HPLC data obtained during this brief condition of stability are included in this table for comparison at similar Ds.

4.2 Steady State Production Analysis

An example of steady state determination is given in Figure 4.1. Here, the NaOH molar flow rate for Run 1, together with the corresponding succinic acid data, are shown. The region marked by “SS” fulfils both steady state criteria discussed in Section 3.5. Between about 90 and 112 h, the absolute average deviation in the NaOH molar flow rate was 2.4%. The corresponding HPLC succinic acid data gave an absolute maximum deviation of 0.8%. Both of these are well within the maximum allowable absolute deviation of 10%.

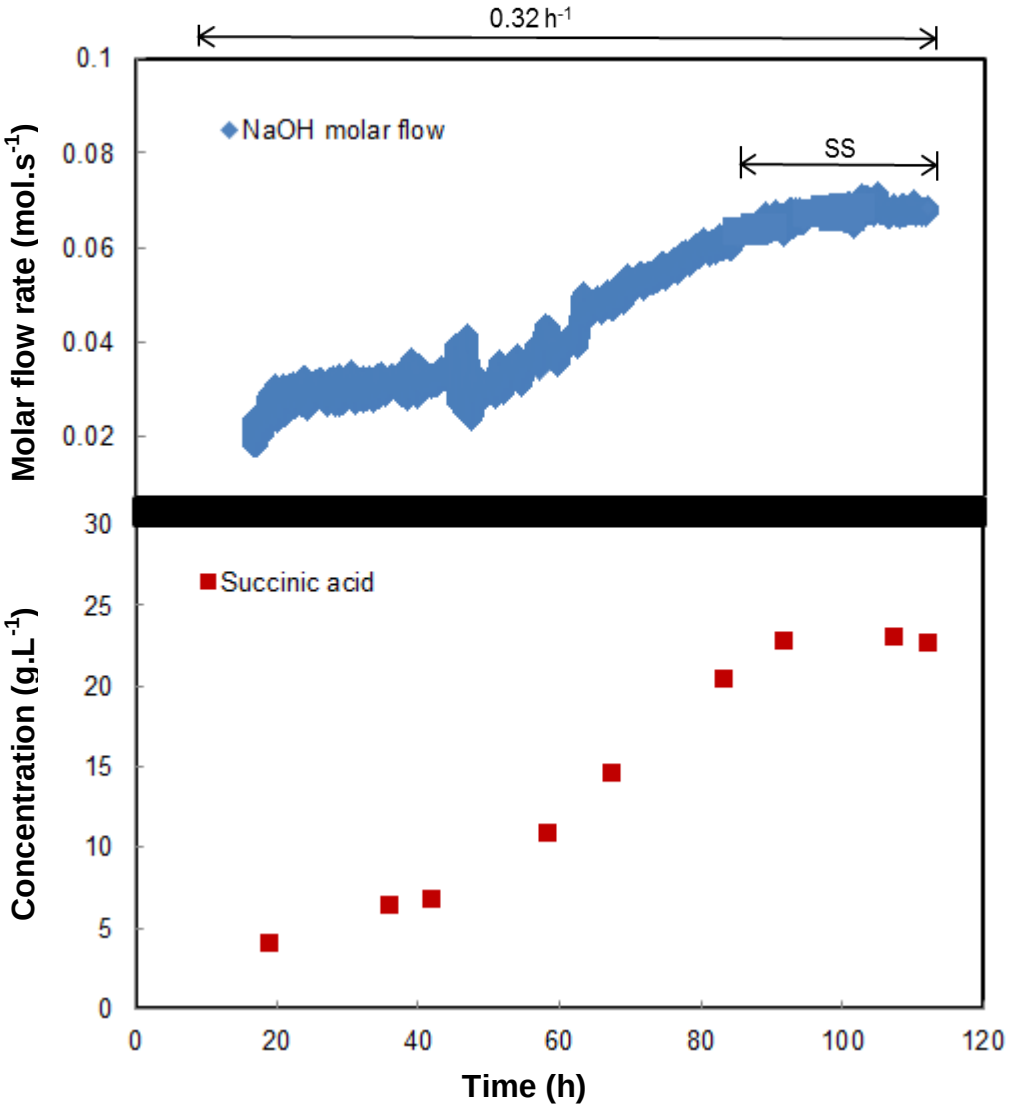

Figure 4.1: *Average molar flow rate of NaOH required to maintain pH over time, and succinic acid concentration profile, with steady state indicated (SS) – Run 1*

4.2.1 Repeatability

The steady state concentrations of the acids produced, glucose consumed and total biomass are shown in Figure 4.2. It can be seen that, for fermentation times < 115 h (see Appendix 2), the total accumulated biomass is apparently independent of dilution rate. Wee *et al.* (2002) had a similar finding, obtaining a total biomass concentration of approximately 80 $g.L^{-1}$ at all dilution rates, using cells immobilised in a hollow fibre reactor. It is suggested that the accumulated biomass displays greater dependence on the available attachment area, since this parameter was kept

constant in all runs. This theory agrees with the mechanism of biofilm growth presented in Section 2.6.1. The biofilm reaches a critical thickness, which is probably determined by the shear rate. Thereafter, parts of the biofilm slough off to colonise new surfaces. If all surfaces are already occupied, the sloughed-off biomass is simply washed out of the system. For reasons outlined in Section 2.6.1, no EPS/cell separations were performed. Of the total biomass collected, only the cell fraction could potentially serve as biocatalyst.

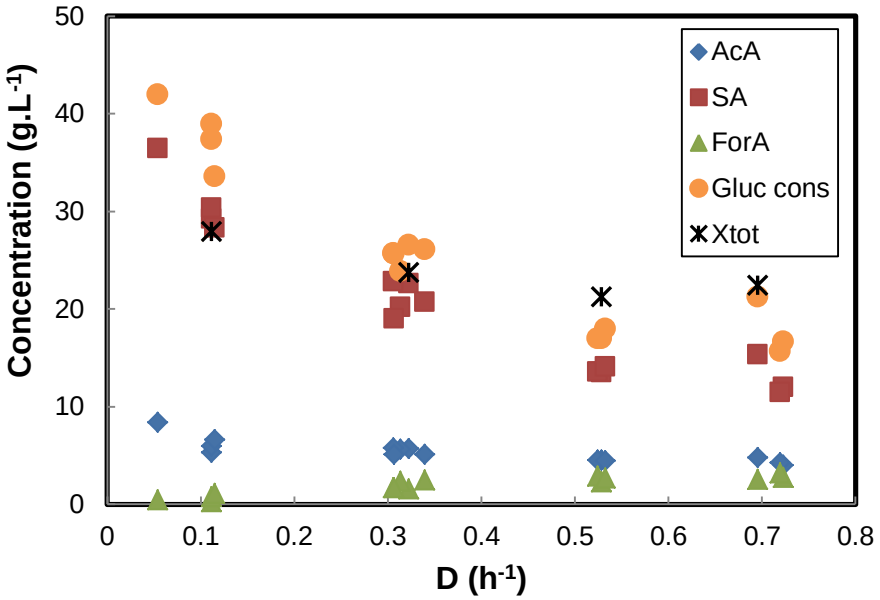

Figure 4.2: *Steady state concentrations at different dilution rates*

Total biomass quantifications (TBQs) at steady state were performed for Runs 1, 3 and 4.The total biomass determined for Run 6 (D = 0.52 h^{-1}) was obtained after the system had experienced significant sloughing off of biomass, and was in the process of rapidly re-establishing itself (Appendix 2). TBQs were not repeated at a given dilution rate due to the time constraints of the project. Figure 4.3 shows the reactor with the mature biofilm grown on Poraver® support particles.

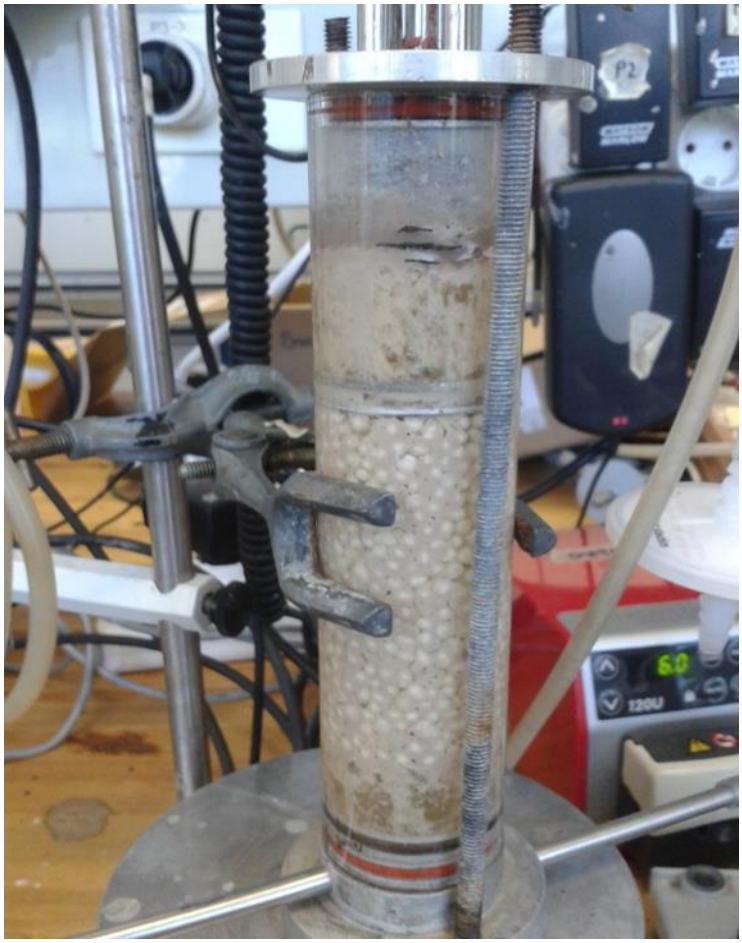

Figure 4.3: *Reactor with mature biofilm during a steady state at D = 0.32 h^{-1} (S_o = 35 $g.L^{-1}$)*

Figure 4.2 shows that the concentrations of the acids produced at a given dilution rate are repeatable at D = ± 0.11 h^{-1}, 0.32 h^{-1} and 0.7 h^{-1}. The succinic acid concentrations were used to quantify repeatability at a specific D. A mean succinic acid value was calculated for each D. The absolute maximum percentage deviation from the mean value was then determined. At D = ± 0.11 h^{-1}, a mean succinic acid concentration of 29.3 $g.L^{-1}$ and absolute maximum deviation of 3.6% were achieved. At D = ± 0.32 h^{-1}, a mean titre of 21 $g.L^{-1}$ and maximum deviation of 9.9% were obtained. Finally, at D = ± 0.7 h^{-1}, a higher-than-expected succinic acid value of 15.3 $g.L^{-1}$ caused an 18% deviation from the mean value of 12.9 $g.L^{-1}$. The decline in repeatability as the dilution rate is increased might be attributed to growth playing a bigger role under these conditions, since inhibitory acid titres are lower. Rapid

growth encourages greater oscillations in biofilm growth and sloughing, which would affect acid results, even during steady state. The variation in the consumed glucose values when D = ± 0.11 h^{-1} might be attributed to inaccurate analyses of S_o. Repeatability at D = 0.52 h^{-1} and 0.054 h^{-1} was not assessed, owing to the time constraints of the project.

The excellent repeatability at D = ± 0.11 h^{-1} occurs despite the fact that in Run 4 a steady state at D = 0.72 h^{-1} was first achieved, before decreasing D to 0.11 h^{-1}. Similarly, in Run 5 the final steady state at D = 0.11 h^{-1} came only after operation at D = 0.32 h^{-1}. This indicates that steady state at a given dilution rate is not path-dependent, but rather is a function of the prevailing reactor conditions. In other words, the activity of the biofilm at a given set of conditions does not determine its steady state activity at another set of conditions.

4.2.2 Stability

During Run 7, the long-term stability of the system was assessed. Figure 4.4 is analogous to Figure 4.1 and indicates steady states during Run 7. Note that the dosing profile at D = 0.72 h^{-1} has been omitted. This was because the erratic behaviour of the reactor, indicated by the scatter in the corresponding succinic acid data, produced an equally erratic dosing signal.

Table 4.3 provides the calculated deviations and means used to determine the period for which steady state was maintained. From Table 4.3 it can be seen that a stable system steady state was maintained for > 72 h when D = 0.31 h^{-1}, 0.11 h^{-1} and 0.054 h^{-1}.

From Figure 4.4 it can be seen that during the first steady state (D = 0.31 h^{-1}) the system displays oscillatory behaviour. This is confirmed by Table 4.3 where the absolute maximum deviation based on succinic acid data just exceeds 10%. This suggests that, under these conditions, the growth rate is fast enough to replace dead or sloughed-off biofilm cells. Sudden drops in productivity, associated with sudden

detachment of biofilm chunks, are soon followed by rapid increases in productivity, associated with biofilm re-growth.

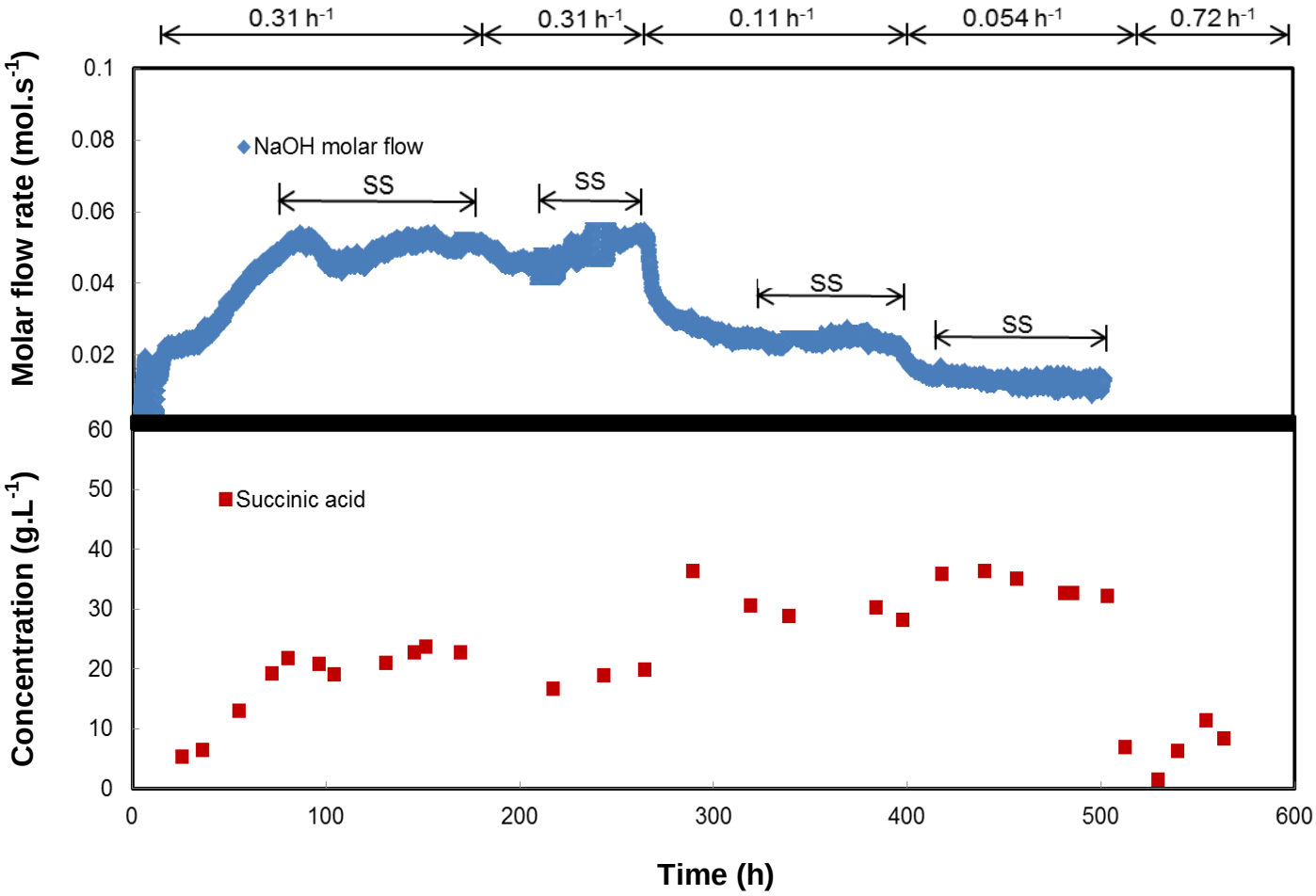

Figure 4.4: *Average molar flow rate of NaOH required to maintain pH over time, and succinic acid concentration profile, with steady states indicated (SS) – Run 7*

Table 4.3: *Calculated parameters in steady state and stability analysis*

D (h)	*AAD in NaOH molar flow (%)[1]*	*AMD in succinic acid titre (%)[2]*	*Steady state duration (h)*
0.31	4.0	10.4	97.14
0.31	6.6	9.7	47.45
0.11	4.3	4.2	78.7
0.054	6.5	5.9	85.2

[1] Calculated by first averaging all NaOH molar flow rate data captured over the steady state period, and then calculating the absolute difference between each of these data points and the mean value. These absolute differences are then averaged over the number of data points used to calculate the mean. This absolute average difference is then expressed as a percentage of the mean value.

[2] Calculated by first averaging all succinic acid data points over the steady state period, and then finding the largest absolute difference between each of these data points and the mean value. This difference is then expressed as a percentage of the mean value.

At D = 0.054 h^{-1}, a period of 85 h has been marked as steady operation, as per the steady state criteria. However, a careful look at the HPLC succinic acid data shows that there is a sudden drop in productivity at about 480 h. After this drop, the expected increase in productivity, associated with a somewhat oscillatory system at higher Ds, does not occur. Similarly, a careful look at the dosing profile at 0.11 h^{-1} shows a distinct drop in the molar flow rate towards the tail-end of the steady state period. The gradual decline in productivity can be attributed to sloughing off of biomass. However, at these low dilution rates, when inhibitory acid concentrations are high, growth is extremely slow and the sloughed-off biomass cannot be replaced.

The effects of cell sloughing can be seen in the suspended cell analysis (Table 4.2) where significantly more biomass is obtained in the outlet at 0.054 h^{-1} than at D = 0.31 h^{-1}. At the higher dilution rate, growth can be expected to be more rapid because of the lower acid concentration. Given that at steady state the rate of cell replacement (or biofilm growth) is equal to that of cell detachment, and assuming that the suspended cells in the system consist solely of detached biofilm cells, the higher D would suggest a higher suspended cell measurement. Since this is not the

case, the suspended cell analysis must include a significant fraction of cells sloughed off without replacement. This biofilm shedding is erratic, so that suspended cell samples collected over 12–24 h at the same dilution rate did not provide repeatable results. This is especially true at the higher dilution rates where stability at a given steady state could not be maintained for long periods. As already mentioned, operation at 0.72 h^{-1} during Run 7 did not result in a stable steady state condition. During the experiment, however, a flat dosing profile was observed for about 6 h (> 4 volume turnovers) at this condition. This would not be seen in Figure 4.4 given the time scale of the run. During the "temporary steady state" observed at D = 0.72 h^{-1}, the succinic acid concentration reached 11.6 $g.L^{-1}$. This agrees with the steady state succinic acid values achieved at a similar dilution rate in previous runs. The approach to this "temporary steady state" when D = 0.72 h^{-1} in Run 7 coincided with aggressive biofilm growth; soon after the "steady state" was reached, however, significant biofilm sloughing occurred. A similar behaviour was observed in Run 6. The data in Appendix 2 show that, following a steady state at D = 0.52 h^{-1}, significant sloughing off of biofilm caused reactor productivity to drop. However, since growth was favourable under these conditions, a rapid increase in succinic acid concentration is seen thereafter.

4.2.3 Specific rates

Figure 4.5 shows the specific rates at different Ds. These calculations were based on steady state volumetric rates and the corresponding total biomass measurement:

$$r_i = \frac{q_i}{X_{tot}} \qquad \textbf{[4.1]}$$

This calculation assumes that the total biomass collected consists of 100% active cells. It can be seen that the specific glucose consumption rate and the organic acid production rates increase with increasing dilution rate.

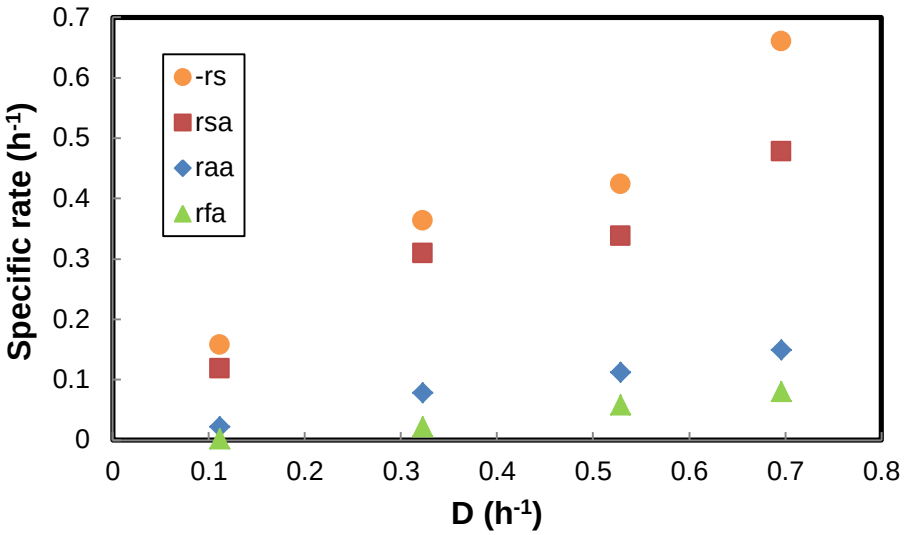

Figure 4.5: *Specific steady state reaction rates at different dilution rates. rs – Specific glucose consumption rate, rsa – Specific succinic acid production rate, raa – Specific acetic acid production rate, rfa – Specific formic acid production rate*

A mass balance over an immobilised cell system at steady state yields

$$D \times x = \mu \times X_{tot} \qquad \textbf{[4.2]}$$

As discussed in Chapter 2, the specific glucose consumption rate can be described by

$$r_s = Y_{xs}^{true} \times \mu + m_s \qquad \textbf{[4.3]}$$

Although the suspended cell analyses in this study were not repeatable, they were low enough such that, when substituted into Equation 4.2, along with corresponding D and average X_{tot} values, μ was small. In fact, μ was usually an order of magnitude lower than the $-r_s$ values in Figure 4.5. According to Equation 4.3 above, this suggests that the growth contribution to the specific rates is negligible. Furthermore, steady state mass balances in which biomass formation was neglected (see Section 3.5) generally showed good agreement between the mass entering and exiting the system. It might therefore be said that the effect of growth-associated

biomass on the overall balance is negligible. This further suggests that μ is small at all dilution rates investigated. A system in which growth effects are almost negligible would suggest a maintenance-driven system:

$$r_s \cong m_s \quad \textbf{[4.4]}$$

It should be noted that, for a maintenance-driven system, the determination of a growth-associated kinetic model is difficult and offers no real insight into the system.

The trend in Figure 4.5 suggests that maintenance is not a constant, as described by Lin *et al.* (2008) and Li *et al.* (2010), but rather a function of the dilution rate (or one of its dependents).

Maintenance has been described as a function of substrate concentration (Villadsen *et al.*, 2011: 289; see Section 2.5.1). According to such a model, a higher *S* value, which is associated with a higher dilution rate, would result in a higher maintenance term. However, according to Figure 4.5, the lowest maintenance is observed at D = 0.11 h^{-1}, where glucose outlet concentrations were similar to those achieved at D = 0.52 h^{-1}. In addition, in Run 7 (Figure 4.4) a dilution rate of 0.31 h^{-1} was maintained while increasing S_o from about 35 $g.L^{-1}$ to 60 $g.L^{-1}$. The higher S_o resulted in a higher *S* of about 30 $g.L^{-1}$. However, the productivity decreased slightly. Based on Equation 4.1, and assuming X_{tot} remains approximately constant, it can be concluded that the specific rates decreased slightly once *S* increased. This is contrary to a substrate-dependent maintenance model.

The description of maintenance as a function of an inhibiting product concentration is far less common. Both Lin *et al.* (2008) and Li *et al.* (2010) mentioned that by-product concentrations, particularly that of formic acid, have a greater inhibitory effect on cell growth than succinic acid. This has been attributed to the negative effects of the acid on the electro-potential gradient of cell membranes. A higher glucose consumption rate would increase the carbon flux to both the ATP-producing

C3 and C4 pathways (see Figure 2.5), which would increase the rate of ATP generation for maintenance.

Alternatively, the effective utilisation of substrate for maintenance purposes may be inhibited by high total acid concentrations, in much the same way as μ is (Corona-González *et al.*, 2008). The higher total acid concentrations at lower Ds might therefore account for the lower maintenance observed under these conditions.

An additional explanation for the trend observed in Figure 4.5 is the deactivation of biocatalyst at low Ds, or cell death. This would compound any differences between specific rates at high and low Ds that arise as a result of differing maintenance contributions. Owing to mass transfer limitations, the deepest biofilm layers would be exposed to the highest inhibitory acid concentrations. This makes the cells found in this region prone to permanent deactivation. However, the dead cells in the internal biofilm layers cannot slough off as easily as surface cells. Therefore, the total biomass collected at the end of a run may consist of a smaller fraction of active cells at lower Ds, where total inhibitory acid concentrations are the highest.

The time to reach steady state when no initial biofilm was present exceeded 35 h at all dilution rates. In Run 4 (Appendix 2) steady state at 0.11 h^{-1} is achieved after about 22 h following the drop in D (Table 4.2) from 0.7 h^{-1}. This demonstrates an extremely rapid system response. This is in contrast to the sluggish response expected as a result of slow growth at the low D. In Run 7 (Appendix 2) a similar trend was observed when the dilution rate was changed from 0.31 h^{-1} to 0.11 h^{-1}, and then further decreased to 0.054 h^{-1}. However, in Run 7, when the D was increased from 0.054 h^{-1} to 0.72 h^{-1}, the expected steady state concentrations (Table 4.2) were only achieved after about 38 h. This is approximately the time taken to reach steady state at D = 0.7 h^{-1} in Runs 3 and 4, in which no attachment had taken place prior to initialisation of this condition. The sluggish response of the system to the increase in D in Run 7 suggests the permanent deactivation of biomass at lower Ds, so that fresh biomass must first be formed before a new steady state is established.

4.3 Analysis of Product Distribution

Figure 4.6 shows the mass ratios of the produced acids as a function of glucose consumed, based on steady and pseudo-steady state results. Lines corresponding to theoretical maximum SA/AA values based on the *pyruvate dehydrogenase* (PDH) and *pyruvate formate lyase* (PFL) pathways (Figure 2.3) respectively have been indicated. A trend line was fitted to SA/AA values based on predicted succinic acid and experimental acetic acid concentrations. The predicted succinic acid concentrations were based on the flux diagram given in Appendix 3. Appendix Experimental formic and acetic acid values were specified. Carbon balances around the PEP and acetate nodes, as well as an NADH balance, were used to solve the various flux distributions. Biomass formation was ignored when calculating all theoretical or predicted values. Note that the experimentally determined glucose consumed is not explicitly specified, since biomass production diverts some of the carbon source away from the glycolysis pathway. The code for the Matlab program used is given in Appendix 3. The predicted SA/AA trend line is bound by the theoretical maximum SA/AA lines.

It can be seen from Figure 4.6 that the predicted SA/AA ratios are lower than the actual SA/AA ratios. In fact, when $\Delta S \geq \sim 35$ g.L^{-1}, SA/AA even exceeds the equivalent maximum PDH-based ratio. The increase in SA/AA with increasing ΔS corresponds to a decrease in FA/AA. This suggests a drop in carbon flux via the C3 pathway. Based on the flux map in Figure III.1, this should result in a decrease in the available redox equivalents for succinic acid production. However, a higher-than-expected succinic acid productivity is maintained. Therefore, based on the discussion in Section 2.3, NADH for succinic acid production must be provided elsewhere. The source of the extra NADH might be a metabolic pathway not usually considered part of *A. succinogenes'* fermentative metabolism. Alternatively, some medium component(s) might provide additional reducing power.

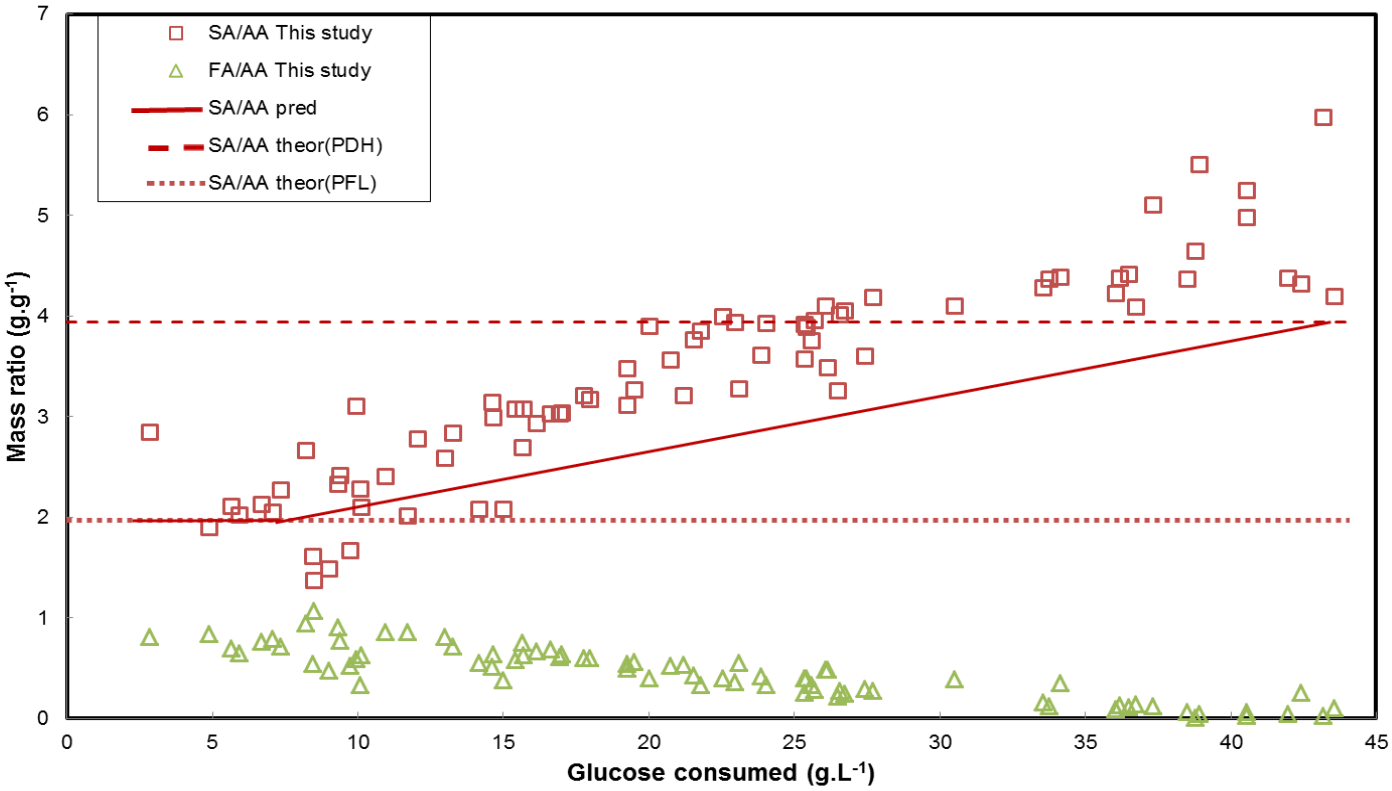

Figure 4.6: *SA/AA and FA/AA mass ratios at different consumed glucose concentrations. SA – succinic acid, AA – acetic acid, FA – formic acid, SA/AA pred – predicted SA/AA mass ratio, SA/AA theor (PDH) – theoretical maximum SA/AA mass ratio, based on the PDH pathway, SA/AA theor (PFL) – theoretical maximum SA/AA mass ratio, based on the PFL pathway*

The proximity of the actual SA/AA ratios to the theoretical PFL line at consumed glucose concentrations less than 15 $g.L^{-1}$ indicates that, under these conditions, PFL is probably the favoured C3 pathway. However, as the values of glucose consumed increase, so does the SA/AA ratio, indicating a shift to the PDH pathway.

The accumulation of the inhibiting acids over time may explain the shift in metabolism over the range of dilution rates studied. Accumulation of formic acid, quoted by many authors (Lin *et al.,* 2008; Li *et al.*, 2010) to be the most detrimental of the acids, may cause the shift from PFL to PDH.

4.4 Comparison with the Literature

Figure 4.7 reproduces Figure 4.6, with the mass ratios obtained by Mwakio (2012) and Van Heerden (2012) also shown. All experimental data may be considered to result from immobilised cell experiments, since biofilm grew on reactor walls in experiments by Van Heerden (2012) and Mwakio (2012). The FA/AA results obtained by these two researchers are very similar to those obtained in this study. There are, however, a few lower-than-expected values obtained by Mwakio (2012) during intentional biofilm experiments. These data points correspond to SA/AA ratios close to the theoretical maximum PDH line. Although Van Heerden (2012) performed similar biofilm experiments, the same trend was not observed. The SA/AA values presented by these authors confirm the shift from the PFL to the PDH pathway at intermediate ΔS values. However, the SA/AA ratios presented in this study tend to be higher. This discrepancy might be attributed to differences in the final medium composition obtained in this study. There were no noteworthy differences between the media described by Mwakio (2012) and Van Heerden (2012), and that used in this study. However, preparation of the medium in this study was different in that clarified corn steep liquor was used. Furthermore, the phosphates were autoclaved separately from the mineral salts and glucose. Both these techniques would have reduced the chance of important nutrients forming complexes during autoclaving. These complexes would otherwise reduce the concentration of nutrients in the medium since they cannot be used by the bacteria in this form. The higher concentrations of freely available nutrients in this study may have been the source of the additional reducing power.

Figure 4.8 compares the steady state glucose consumption rates and succinic acid productivities achieved in this study with those reported in the literature. Note that comparative data have only been included at the range of dilution rates studied.

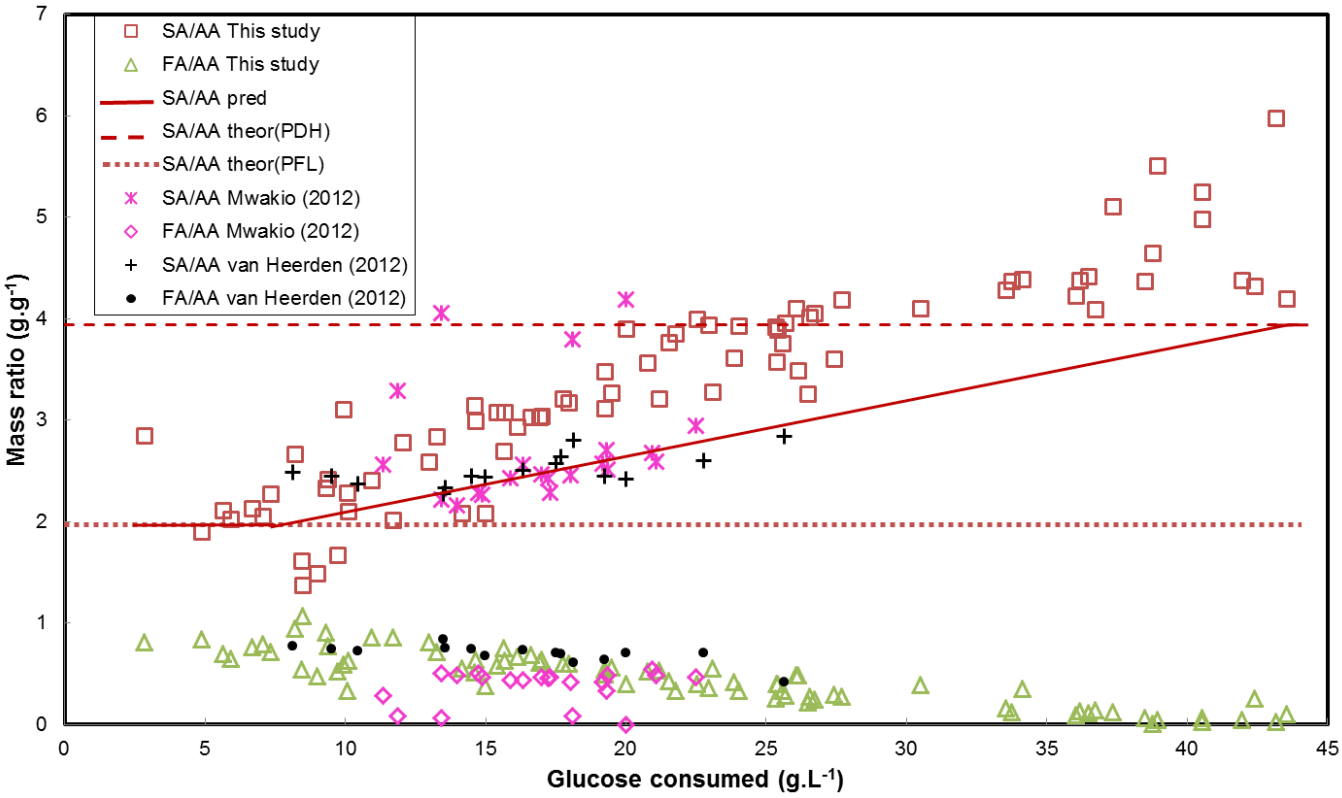

Figure 4.7: *SA/AA and FA/AA mass ratios at different consumed glucose concentrations in this and other studies. SA – succinic acid, AA – acetic acid, FA – formic acid, SA/AA pred – predicted SA/AA mass ratio, SA/AA theor (PDH) – theoretical maximum SA/AA mass ratio, based on the PDH pathway, SA/AA theor (PFL) – theoretical maximum SA/AA mass ratio, based on the PFL pathway*

Yields can be determined by:

$$Y_{SS} = \frac{P_{SA}}{-q_s} \qquad \textbf{[4.5]}$$

Therefore, for similar glucose consumption rates or similar productivities, the longer the dotted line between two points, the lower the yield. Kim *et al.* (2009) achieved yields of between 0.5 and 0.59 $g.g^{-1}$ using cell recycle and S_o = 60 $g.L^{-1}$. These values are much lower than those achieved in this study, even at a D of about 0.1 h^{-1}, where equivalent glucose feed concentrations were used. The glucose consumption rates and productivities achieved by Van Heerden (2012) and Mwakio

(2012) are similar, but are lower than those achieved in this study. This is despite the fact that both authors used S_o = 20 and 40 g.L^{-1} in their fermentations, compared with 35 g.L^{-1} used throughout most of this study. This suggests that the higher reaction rates achieved in this study are independent of the differences in initial glucose concentration. Note that data obtained by Mwakio (2012) and Van Heerden (2012) during intentional biofilm runs are included in Figure 4.8. The highest productivity achieved in this study was 10.7 g.L^{-1}.h^{-1}, at a D of about 0.7 h^{-1}. However, the highest succinic acid productivity reported to date was 14.8 g.L^{-1} per hour, achieved in a cell recycle reactor by Meynial-Salles *et al.* (2008), using *A. succiniproducens*.

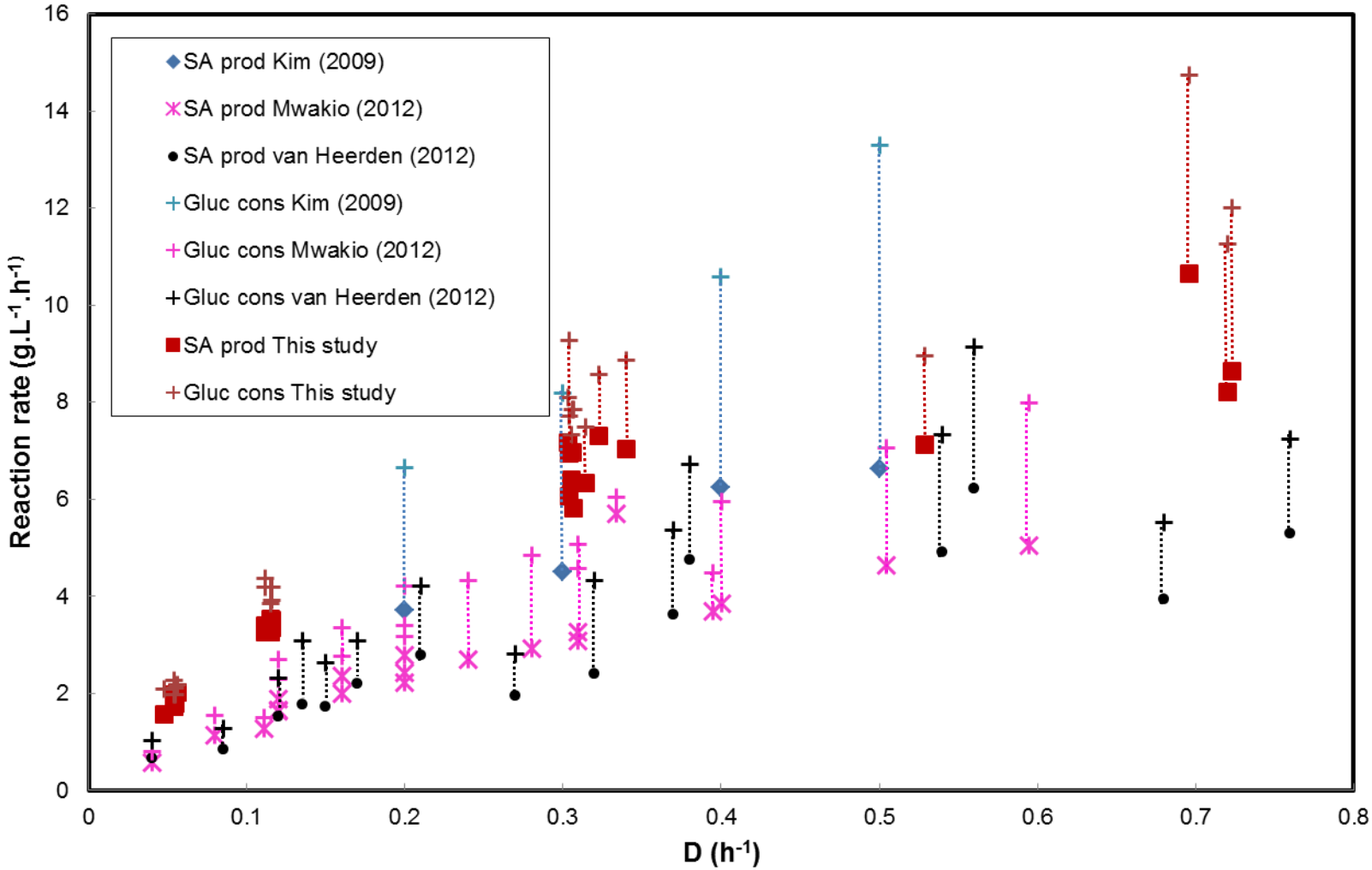

Figure 4.8: *Succinic acid productivities and glucose consumption rates compared with those in other studies. SA prod – Succinic acid productivity, Gluc cons – Glucose consumption rate*

Chapter 5 Conclusions and Recommendations

A. succinogenes was immobilised on Poraver® supports during continuous succinic acid fermentation. Dilution rates of 0.054 to 0.72 h^{-1} were investigated. The highest yields exceeded 0.85 $g.g^{-1}$ and the highest productivity obtained was 10.7 $g.L^{-1}.h^{-1}$ at D = 0.7 h^{-1}.

Steady state succinic, acetic and formic acid and glucose concentrations proved to be repeatable at a given dilution rate. Furthermore, the system was able to maintain a stable steady state for more than 72 h at dilution rates ≤ 0.31 h^{-1}. The longest steady state period was maintained for about 97 h at D = 0.31 h^{-1}, during which slight oscillations in productivity occurred. At lower dilution rates, a slow decline in productivity was observed for time periods longer than about 75 h. This may be attributed to poor growth caused by high inhibitory acid titres. When growth is severely inhibited, cells that slough off from the biofilm are unable to be replaced. This was confirmed by higher-than-expected suspended cell measurements obtained at low dilution rates. The decline in productivity may also be attributed to a slow deactivation of cells in the biofilm. This was supported by the time required to establish a steady state following a dramatic increase in dilution rate, which suggested significant growth of fresh biofilm during the transition. At dilution rates higher than 0.31 h^{-1}, a steady state could not be maintained for long periods. This was because, at the lower acid titres observed, growth was favoured, which tended to make the biofilm unstable. Severe biofilm sloughing would follow periods of aggressive biofilm growth, so that suspended cell analyses based on large-volume product samples showed poor repeatability.

It was found that the amount of accumulated biomass at steady state was independent of the dilution rate for fermentation times < 115 h. It was suggested that the biomass quantity was instead dependent on the available attachment area. Total

biomass was used to determine specific rates in order to gain insight into the system kinetics. The specific rate calculation assumed 100% active biomass. Specific rates were found to increase with increasing dilution rate. This trend was explained by a maintenance-driven system, in which growth was negligible.

Growth was shown to be severely inhibited throughout this study, since suspended cell measurements were small (< 3 $g.L^{-1}$). These suspended cell measurements yielded μ values about an order of magnitude smaller than the calculated specific glucose consumption rates, suggesting that under these conditions, growth is indeed negligible. Furthermore, mass balances ignoring biomass formation suggested that the growth-related biomass contribution was minimal. Therefore, the system was considered to be maintenance driven. Based on this premise, maintenance could not be considered as a constant, but, rather, dependent on the acid concentrations. It was possible that the severely inhibiting effects of high formic acid titres at high Ds resulted in greater maintenance requirements. Alternatively, the high total inhibitory acid concentrations at low Ds may have resulted in inefficient substrate consumption for maintenance purposes.

Furthermore, the permanent deactivation of cells was observed at high acid titres. This provides the possibility of an additional explanation for the observed trend in Figure 4.5. Any differences between the specific rates obtained at high and low dilution rates as a result of different maintenance contributions would have been exacerbated by this phenomenon. The deeper biofilm layers are prone to cell death as a result of the high acid concentrations experienced in these regions. However, the system cannot easily rid itself of dead cells in the deeper biofilm layers. Therefore, the total biomass collected at the end of the run may consist of a significant fraction of inactive cells. This fraction may increase as the dilution rate decreases and the total acid concentration increases.

Product distribution analysis was based on Figure III.1. Known *A. succinogenes* metabolism involves the reduction of phosphoenolpyruvate (PEP) to succinate. The required reducing power is provided by the simultaneous oxidation of PEP to

acetate. It was found that at high values of glucose consumed, the SA/AA mass ratio exceeded the maximum theoretical ratio of 3.94 $g.g^{-1}$, calculated by redox balancing. A maximum steady state SA/AA of 5.51 $g.g^{-1}$ at 0.11 h^{-1} was obtained. This suggests that there must be some unknown source of additional NADH. This could be either an additional metabolic pathway or some medium component(s). The higher-than-expected SA/AA ratio goes hand-in-hand with a lower-than-expected FA/AA ratio. This indicates that, under these conditions, carbon flux to the C3 pathway is reduced. At lower values of glucose consumed (ΔS< 15 $g.L^{-1}$), the pyruvate formate lyase (PFL) pathway was the preferred oxidative route, while at higher values of glucose consumed, the pyruvate dehydrogenase (PDH) pathway was favoured. Succinic acid yields were at their lowest when oxidation via the PFL pathway was the only active C3 route. Higher SA/AA ratios (and consequently, better yields) were obtained in this study compared with those obtained by Van Heerden (2012) and Mwakio (2012). This may be attributed to differences in medium preparation, which involved reducing the possibility of nutrient complexation.

A growth-associated kinetic model could not be obtained in this study because the system proved to be maintenance driven. It is therefore recommended that any further kinetic research should focus on identifying the process variables that affect maintenance. The relative activity of the biofilm at different dilution rates should also be quantified in order to dissociate the effects of cell death and maintenance. Further research should be conducted into the effects of different media components and their preparation in order to identify the unknown source of NADH.

It is advised that any process utilising immobilised *A. succinogenes* cells in a continuous reactor should operate at an intermediate D. Under these conditions, growth is rapid enough to replace detached or deactivated cells, but is slow enough to avoid severe oscillatory behaviour. Good productivities and yields are also obtained under the influence of the PDH pathway. It is also recommended that precautions be taken during medium preparation, so as to reduce the possibility of nutrient complexation.

Chapter 6 References

Annenberg Foundation (2013) Biofilm formation and bacterial communication. Available at: http://www.learner.org/courses/biology/textbook/microb/microb_10.html [accessed on 24 September 2013].

Baltaru, R, Galaction, AI and Caşcaval, D (2009) Bioreactors of 'basket' type with immobilized biocatalysts. Paper presented at *The 2nd WSEAS International Conference on Biomedical Electronics and Biomedical Informatics*, 20–22 August 2009, Moscow, Russia.

Bastidon, AI (2012) *Biosuccinic acid*. Report, Nexant's CHEMSYSTEMS Process Evaluation/ Research Planning (PERP) Program.

Beauprez, JJ, De Mey, M and Soetaert, WK (2010) Microbial succinic acid production: Natural versus metabolic engineered producers. *Process Biochemistry*, 45(7): 1103–1114.

Bechthold, I, Bretz, K, Kabasci, S, Kopitzky, R and Springer, A (2008) Succinic acid: A new platform chemical for bio-based polymers from renewable resources. *Chemical Engineering and Technology*, 31(5): 647–654.

Chemicals Technology (2012) Reverdia's bio-based succinic acid plant, Italy. Available at: http://www.chemicals-technology.com/projects/reverdia-bio-based-succinic-acid-plant-italy/ [accessed on 29 August 2013].

Corona-González, RI, Bories, A, González-Álvarez, V and Pelayo-Ortiz, C (2008) Kinetic study of succinic acid production by *Actinobacillus succinogenes* ZT-130. *Process Biochemistry*, 43(10): 1047–1053.

Cukalovic, A and Stevens, CV (2008) Feasibility of production methods for succinic acid derivatives : a marriage of renewable resources and chemical technology *Biofuels, Bioproducts and Biorefining*, 6(2): 505–529.

Dennert Poraver GmbH (2012) Poraver® expanded glass: Technical data sheet. Available at: http://poraver.com/sites/default/files/download/121130_Poraver_TD _ EN_0.pdf [accessed on 28 August 2013].

Flickinger, M and Drew, S (1999) *Encyclopedia of Bioprocess Technology – Fermentation, Biocatalysis, and Bioseparation, Volumes 1–5*. New York: Wiley.

Galaction, AI, Kloetzer, L, Turnea, M, Webb, C, Vlysidis, A and Caşcaval, D (2012) Succinic acid fermentation in a stationary-basket bioreactor with a packed bed of immobilized *Actinobacillus succinogenes*: 1. Influence of internal diffusion on substrate mass transfer and consumption rate. *Journal of Industrial Microbiology and Biotechnology*, 39(6): 877–888.

Geraili, A, Sharma, P, Willis, R and Romagnoli, JA (2013) A simulation and techno-economic optimization-based methodology to design multi-product lignocellulosic biorefineries. *Chemical Engineering Transactions*, 32: 1183–1188.

Guettler, MV, Jain, MK and Soni, BK (1996) Process for making succinic acid, microorganisms for use in the process and methods of obtaining the microorganisms. *US Patent 5,723,322*, assigned to Michigan Biotechnology Institute, US.

Habibi, N, Soleimanian-Zad, S and Zeinoddin, M (2011) Exopolysaccharides produced by pure culture of *Lactobacillus*, *Lactococcus* and yeast isolated from kefir grain by microtiter plate assay: Optimization and comparison. *World Applied Sciences Journal*, 12(6): 742–750.

Hager, S (2013) Myriant achieves major milestone: Successful start-up at flagship bio-succinic acid plant in Lake Providence, LA. Available at: http://www.myriant.com/med ia/press-releases/myriant-achieves-successful-start-up-at-lake-providence-la-plant.cfm [accessed on 28 August 2013].

Hatzikioseyian, A and Remoundaki, E (*sine anno*) Multiphase reactors – Reactor configurations for biofilm reactors/immobilized cell reactors. Available at:

http://www.metal. ntua.gr/~pkousi/e-learning/bioreactors/page_08.htm [accessed on 25 September 2013].

Higson, A (2013) Platform chemicals – Renewable chemicals factsheet: Succinic acid. Available at: http://www.nnfcc.co.uk/publications/nnfcc-renewable-chemicals-factsheet-succinic-acid [accessed on 24 September 2013].

HyCa Technologies Pvt. Ltd. (2013) Biofouling: Steps in biofilm formation. Available at: http://www.hycator.com/domain/functional-sectors/ biofouling/steps-in-biofilm-formation.html [accessed on 24 September 2013].

Jantama, K, Haupt, MJ, Svoronos, SA, Zhang, X, Moore, JC, Shanmugam, KT and Ingram, LO (2008) Combining metabolic engineering and metabolic evolution to develop non-recombinant strains of *Escherichia coli* C that produce succinate and malate. *Biotechnology and Bioengineering*, 99(5): 1140–1153.

Kim, MI, Kim, NJ, Shang, L, Chang, YK, Lee, SY and Chang, HN (2009) Continuous production of succinic acid using an external membrane cell recycle system. *Journal of Microbiology and Biotechnology*, 19(11): 1369–1373.

Lane, J (2012) Myriant: Biofuels Digest's 5-Minute Guide. Available at: http://www. biofuel sdigest.com/bdigest/2012/11/19/myriant-biofuels-digests-5-minute-guide/ [accessed on 28 August 2013].

Lee, PC, Lee, SY and Chang, HN (2009) Kinetic study of organic acid formations and growth of *Anaerobiospirillum succiniciproducens* during continuous cultures. *Journal of Microbiology and Biotechnology*, 19(11): 1379–1384.

Li, Q, Wang, D, Wu, Y, Yang, M, Li, W, Xing, J and Su, Z (2010) Kinetic evaluation of products inhibition to succinic acid producers *Escherichia coli* NZN111, AFP111, BL21 and *Actinobacillus succinogenes* 130Z^{T}. *Journal of Microbiology*, 48(3): 290–296.

Lin, SKC, Du, C, Koutinas, A, Wang, R and Webb, C (2008) Substrate and product inhibition kinetics in succinic acid production by *Actinobacillus succinogenes. Biochemical Engineering Journal*, 41(2): 128–135.

Liu, H and Fang, HHP (2002) Extraction of extracellular polymeric substances (EPS) of sludges. *Journal of Biotechnology*, 95(3): 249–256.

Lucintel (2012) Global polymer industry 2012–2017: Trend, profit, and forecast analysis. Available at http://www.lucintel.com/reports/chemical_composites /global_polymer_industry_2012_2017_trends_foreacast_june_2012.aspx [accessed on 23 September 2013].

Maiorella, B, Blanch, HW and Charles, RW (1983) By-product inhibition effects on ethanolic fermentation by *Saccharomyces cerevisiae. Biotechnology and Bioengineering*, 25(1): 1–10.

McKinlay, JB, Vieille, C and Zeikus, JG (2007) Prospects for a bio-based succinate industry. *Applied Microbiology and Biotechnology*, 76(4): 727–740.

McKinlay, JB and Vieille, C (2008) 13C-metabolic flux analysis of *Actinobacillus succinogenes* fermentative metabolism at different $NaHCO_3$ and H_2 concentrations. *Metabolic Engineering*, 10(1): 55–68.

McKinlay, JB, Laivenieks, M, Schindler, BD, McKinlay, AA, Siddaramappa, S, Challacombe, JF, Lowry, SR, Clum, A, Lapidus, AL, Burkhart, KB, Harkins, C, Vieille, C (2010) A genomic perspective on the potential of *Actinobacillus succinogenes* for industrial succinate production. *BMC Genomics*, 11(1): 680–696.

Meynial-Salles, I, Dorotyn, S and Soucaille, P (2008) A new process for the continuous production of succinic acid from glucose at high yield, titer and productivity. *Biotechnology and Bioengineering*, 99(1): 129–135.

Mwakio, J (2012) *Continuous succinic acid production by* Actinobacillus succinogenes*: Suspended cell and biofilm studies in an anaerobic slurry reactor.* Master's Thesis, Department of Chemical Engineering, University of Pretoria.

Mynewsdesk (2013) World succinic acid market will climb above USD 836.2 million in 2018 : Transparency Market Research. Available at: http://www.mynews desk.com /us/view/news/world-succinic-acid-market-will-climb-above-usd-836-

2-million-in-2018-transparency-market-research-65767 [accessed on 22 September 2013].

Nuijten, S (2012) BASF and CSM establish 50-50 joint venture for bio-based succinic acid. Available at: http://basf.com/group/pressrelease/P-12-444 [accessed on 29 August 2013].

Ostling, CE and Lindgren, SE (1993) Inhibition of enterobacteria and *Listeria* growth by lactic, acetic and formic acids. *Journal of Applied Bacteriology*, 75(1): 18–24.

Pan, X, Liu, J, Zhang, D, Chen, X, Li, L, Song, W and Yang, J (2010) A comparison of five extraction methods for extracellular polymeric substances (EPS) from biofilm by using three- dimensional excitation-emission matrix (3DEEM) fluorescence spectroscopy. *Water SA*, 36(1): 2535–2554.

Pereira, MA, Alves, MM, Azeredo, J, Mota, M and Oliveira, R (2000) Influence of physico-chemical properties of porous microcarriers on the adhesion of an anaerobic consortium. *Journal of Industrial Microbiology and Biotechnology*, 24(3): 181–186.

Perry, R, Green, D and Maloney, J (1997) *Perry's Chemical Engineers' Handbook*, 7th ed. New York: McGraw-Hill.

Plank, J (2012) Doesn't play well with others – The chemistry of the autoclave. Available at: http://bitesizebio.com/articles/doesn't-play-well-with-others-the-chemistry-of-the-autoclave/ [accessed on: 28 August 2013].

Samuelov, NS, Lamed, R, Lowe, S and Zeikus, JG (1991) Influence of CO_2-HCO_3 levels and pH on growth, succinate production, and enzyme activities of *Anaerobiospirillum succiniciproducens. Applied and Environmental Microbiology*, 57(10): 3013–3019.

Sánchez, AM, Bennett, GN, San, KY (2005) Novel pathway engineering design of the anaerobic central metabolic pathway in *Escherichia coli* to increase succinate yield and productivity. *Metabolic Engineering*, 7: 229–239.

Sarika, AR, Lipton, AP and Aishwarya, MS (2012) Comparative assessment of bacteriocin production in free and immobilized *Lactobacillus plantarum* MTCC B1746 and *Lactococcus lactis* MTCC B440. *Journal of Applied Sciences Research*, 8(4): 2197–2202.

Sauer, M, Porro, D, Mattanovich, D and Branduardi, P (2008) Microbial production of organic acids: Expanding the markets. *Trends in Biotechnology*, 26(2): 100–108.

Sheridan, K (2011) BioAmber and Mitsui & Co. to build and operate plants producing succinic acid and BDO. Available at: http://investor.bioamber.com/phoenix.z html ?c=250878&p=irol-newsArticle&ID=1684035&highlight= [accessed on 29 August 2013].

Sikyta, B. (1995) *Techniques in Applied Microbiology.* Prague: Elsevier.

Song, H and Lee, SY (2006) Production of succinic acid by bacterial fermentation. *Enzyme and Microbial Technology*, 39(3): 352–361.

Suja, F and Donnelly, T (2006) Reynolds number calculation method for aerobic biological porous packed reactors. *Jurnal Kejuruteraan (Journal of Engineering)*, 18: 21–28.

Sutherland, I (2001) Biofilm exopolysaccharides: A strong and sticky framework. *Microbiology*, 147(1): 3–9.

Tampion, J and Tampion, M (1987) *Immobilized Cells: Principles and Applications*. Cambridge: Cambridge University Press.

University of Glasgow (2011) Biofilms. Available at: http://2011.igem.org/Team: Glasgow /Biofilm [accessed on 24 September 2013].

Urbance, SE, Pometto, AL, DiSpirito, AA and Demirci, A (2003) Medium evaluation and plastic composite support ingredient selection for biofilm formation and succinic acid production by *Actinobacillus succinogenes. Food Biotechnology*, 17(1): 53–65.

Urbance, SE, Pometto, AL, DiS, AA and Denli, Y (2004) Evaluation of succinic acid continuous and repeat-batch biofilm fermentation by *Actinobacillus succinogenes* using plastic composite support bioreactors. *Applied Microbiology and Biotechnology*, 65(6): 664–670.

Van Heerden, CD (2012) *Continuous succinic acid fermentation by* Actinobacillus succinogenes. Master's Thesis, University of Pretoria.

Van Heerden, CD and Nicol, W (2013) Continuous and batch cultures of *Escherichia coli* KJ134 for succinic acid fermentation: Metabolic flux distributions and production characteristics. *Microbial Cell Factories*, 12(1): 1–10. Villadsen, J, Nielsen, J and Lidén, G (2011) *Bioreaction Engineering Principles*, 3rd ed. New York: Springer.

Vemuri, GN, Eiteman, MA and Altman, E (2002) Effects of growth mode and pyruvate carboxylase on succinic acid production by metabolically engineered strains of *Escherichia coli. Applied and Environmental Microbiology*, 68(4): 1715–1727.

Vu, B, Chen, M, Crawford, RJ and Ivanova, EP (2009) Bacterial extracellular polysaccharides involved in biofilm formation. *Molecules*, 14(7): 2535–2554.

Wee, YJ, Yun, JS, Kang, KH and Ryu, HW (2002) Continuous production of succinic acid by a fumarate-reducing bacterium immobilized in a hollow-fiber bioreactor. *Applied Biochemistry and Biotechnology*, 98–100(2): 1093–1104.

Zeikus, JG, Jain, MK and Elankovan, P (1999) Biotechnology of succinic acid production and markets for derived industrial products. *Applied Microbiology and Biotechnology*, 51(5): 545–552.

I. Appendix 1

a)

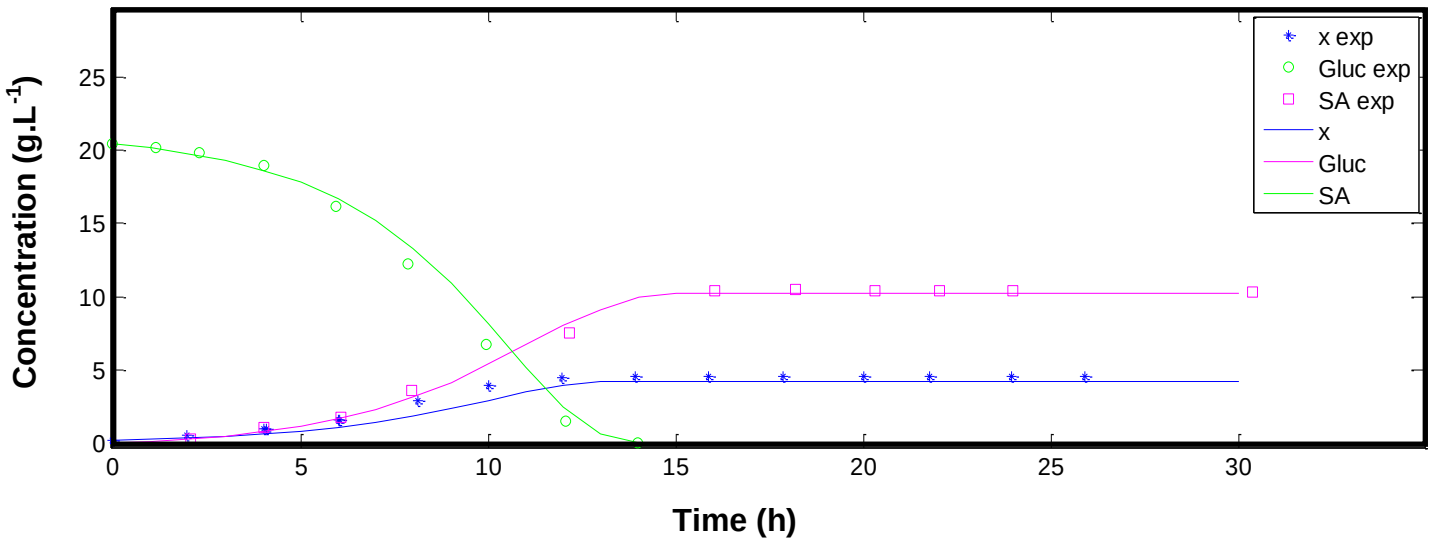

b)

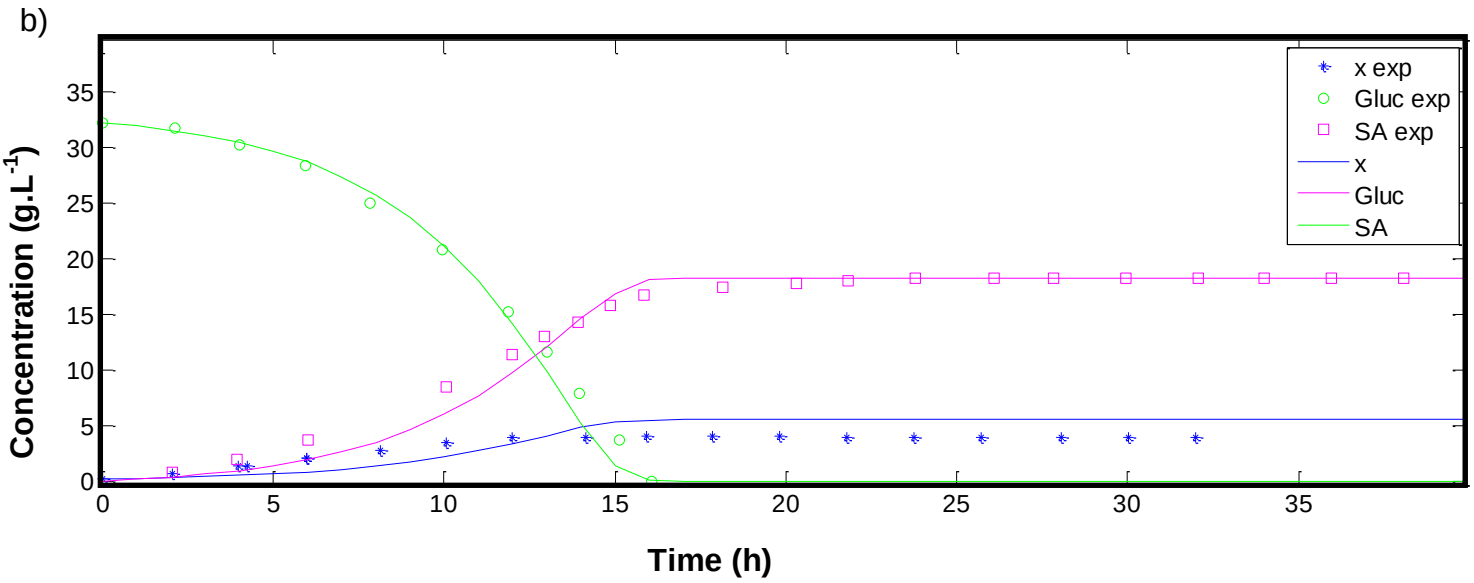

c)

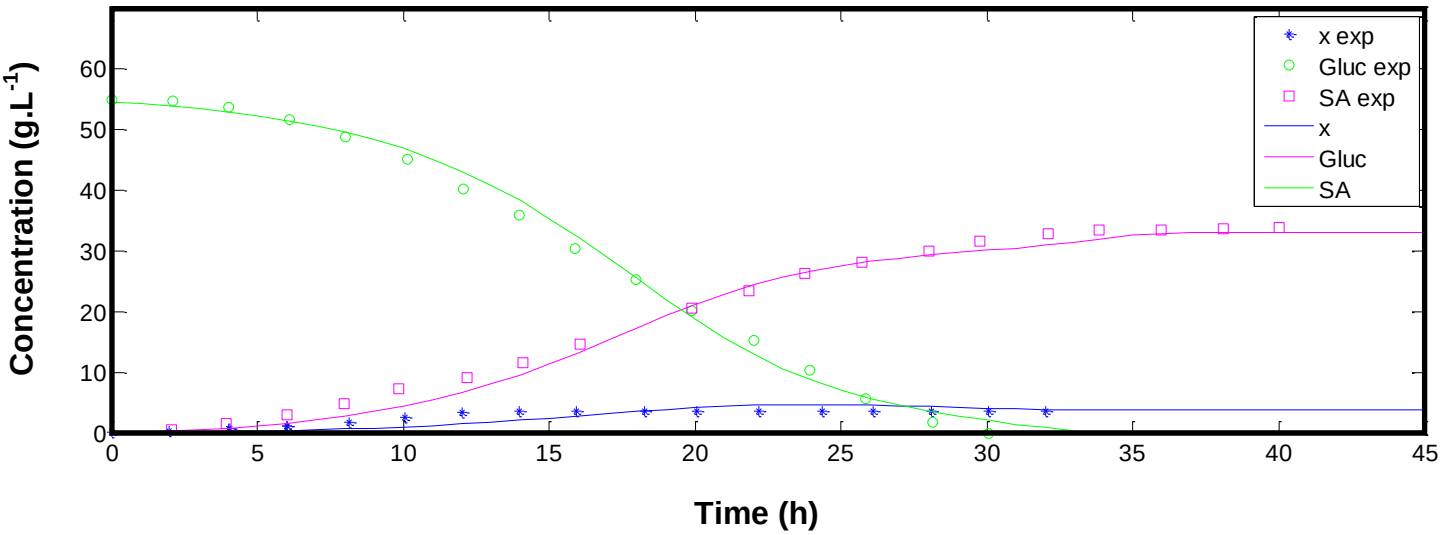

Figure I.1: *Kinetic modelling of experimental data obtained by Corona-González* et al. *(2008) in batch fermentations. a) S_o = 20.4 g.L^{-1}, b) S_o = 32.2 g.L^{-1} & c) S_o = 54.7 g.L^{-1}. x exp – experimental suspended cell concentration, Gluc exp – experimental glucose concentration & SA exp – experimental succinic acid concentration. x – suspended cell concentration predicted by the model, Gluc – glucose concentration predicted by the model, SA – succinic acid concentration predicted by the model*

II. Appendix 2

Table II.1: *Results from all fermentations*

D (h^{-1})	*Dosing[1] (%)*	*S_o ($g.L^{-1}$)*	*$S_{o,adj}$[2] ($g.L^{-1}$)*	*S ($g.L^{-1}$)*	*Succinic formed ($g.L^{-1}$)*	*Acetic formed ($g.L^{-1}$)*	*Formic formed ($g.L^{-1}$)*	*P_{SA} ($g.L^{-1}.h^{-1}$)*	*Y_{SS}[3] ($g.g^{-1}$)*	*% Mass accounted for*	*% Volume accounted for[4]*	*Time[5] (h)*
						Run 1						
0.312	3.2	38.1	36.9	28.4	3.9	2.9	3.1	1.2	0.47	97.0	78	19.3
0.313	3.6	38.1	36.7	28.3	6.4	3.9	2.1	2.0	0.75	105.2	87	36.1
0.314	3.9	38.1	36.6	26.9	6.7	4.0	2.1	2.1	0.69	102.5	125	42.2
0.316	4.7	38.1	36.3	21.3	10.7	5.1	2.0	3.4	0.72	101.0	107.2	58.7
0.318	6.0	38.1	35.8	16.6	14.5	4.7	2.5	4.6	0.75	97.6	119	67.8
0.322	7.4	38.1	35.3	10.0	20.3	5.7	2.3	6.5	0.80	97.6	119	83.6
0.323	7.6	36.5	33.7	6.3	22.7	6.3	1.9	7.3	0.83	99.3	115	91.9
0.323	7.6	36.5	33.7	6.0	23.0	5.5	1.5	7.4	0.83	96.2	118	107.5
0.323	7.7	36.5	33.7	7.2	22.6	5.6	1.6	7.3	0.85	99.2	122	112.4
						Run 2						
0.311	3.9	35.9	34.5	25.5	6.6	4.4	2.1	2.0	0.73	105.6	129	45.7
0.319	6.0	35.9	33.8	14.5	15.4	4.4	2.2	4.9	0.80	98.8	120	69.1
0.32	6.3	35.9	33.7	10.7	18.9	4.8	1.8	6.0	0.82	97.6	110	80.8
0.322	7.1	35.9	33.4	6.9	22.4	6.9	1.5	7.2	0.84	102.3	113	96.9
0.317	5.6	36.6	34.6	24.5	8.5	3.7	1.2	2.7	0.84	104.6	121	118.9
0.302	5.5	36.6	34.6	20.5	9.8	4.7	2.6	3.0	0.70	100.6	104.6	154.2

D (h^{-1})	Dosing[1] (%)	S_o ($g.L^{-1}$)	$S_{o,adj}$[2] ($g.L^{-1}$)	S ($g.L^{-1}$)	Succinic formed ($g.L^{-1}$)	Acetic formed ($g.L^{-1}$)	Formic formed ($g.L^{-1}$)	P_{SA} ($g.L^{-1}.h^{-1}$)	Y_{SS}[3] ($g.g^{-1}$)	% Mass accounted for	% Volume accounted for[4]	Time[5] (h)
0.326	6.9	36.6	34.1	11.0	17.9	5.5	3.0	5.8	0.78	97.9	98.5	166.1
0.332	7.4	36.6	33.9	7.8	19.5	5.6	2.7	6.5	0.74	93.1	97.5	171.9
0.34	6.8	36.6	34.1	8.1	20.7	5.1	2.5	7.0	0.79	94.9	104.1	189.6
						Run 3						
0.695	2.5	36.4	35.5	29.6	5.4	2.7	1.7	3.8	0.91	106.0	102.6	36.4
0.706	3.5	36.4	35.1	25.0	9.1	4.4	2.7	6.5	0.90	109.4	102.2	41.9
0.708	4.4	36.4	34.8	19.4	12.7	4.1	2.4	9.0	0.83	102.5	102.7	52.1
0.697	4.9	36.7	34.9	15.4	14.3	4.4	2.5	10.0	0.73	95.4	105.1	69.6
0.696	5.1	36.7	34.8	13.7	15.3	4.8	2.5	10.7	0.72	94.4	105.5	84.4
						Run 4						
0.711	1.7	37.2	36.5	31.7	2.4	1.3	1.1	1.7	0.49	97.0	101.4	6.3
0.712	2.8	37.2	36.1	26.8	6.0	2.6	2.3	4.3	0.64	98.3	102.3	23.1
0.719	3.5	37.2	35.9	22.9	9.0	3.5	2.8	6.5	0.70	98.4	102	29.7
0.723	4.0	37.2	35.7	19.1	12.0	3.9	2.7	8.6	0.72	96.7	101.9	45.7
5.3	0.7	61.5	61.1	57.8	1.6	0.7	0.5	8.6	0.49	98.3	n/a	47.2
0.115	9.8	61.5	55.5	13.1	32.7	7.6	2.0	3.8	0.77	90.7	n/a	54.0
0.113	8.0	61.5	56.6	13.4	36.8	6.2	0.1	4.2	0.85	92.5	n/a	69.7
0.113	7.4	61.5	56.9	16.4	30.6	5.8	0.1	3.5	0.76	91.7	93.1	76.1
0.112	7.0	61.5	57.2	18.3	29.2	5.3	0.3	3.3	0.75	86.7	95.1	90.5
						Run 5						
0.305	2.6	37.2	36.3	29.2	5.2	2.6	2.0	1.6	0.74	102.2	99.8	23.8

$D\ (h^{-1})$	*Dosing*[1] *(%)*	$S_o\ (g.L^{-1})$	$S_{o,\ adj}$[2] $(g.L^{-1})$	$S\ (g.L^{-1})$	*Succinic formed* $(g.L^{-1})$	*Acetic formed* $(g.L^{-1})$	*Formic formed* $(g.L^{-1})$	$P_{SA}\ (g.L^{-1}.h^{-1})$	Y_{SS}[3] $(g.g^{-1})$	*% Mass accounted for*	*% Volume accounted for*[4]	*Time*[5] *(h)*
0.321	3.2	37.2	36.0	26.7	7.4	3.1	2.4	2.4	0.79	102.9	95.6	42.2
0.302	4.7	37.2	35.5	19.8	12.4	4.0	2.5	3.7	0.79	98.9	102.8	58.7
0.314	5.7	37.2	35.1	14.4	16.7	4.7	2.5	5.3	0.81	99.0	103	70.2
0.314	6.0	37.2	35.0	11.2	20.2	5.6	2.3	6.3	0.85	101.3	100.5	90.8
0.313	3.1	37.2	36.1	21.4	11.6	3.9	2.5	3.6	0.79	100.8	n/a	97.3
0.313	4.9	37.2	35.4	17.7	13.8	4.3	2.6	4.3	0.78	99.1	n/a	101.6
0.109	8.0	58.1	53.5	19.3	25.7	5.8	2.0	2.8	0.75	91.0	103.6	142.5
0.112	7.5	58.1	53.7	16.4	30.3	5.9	0.8	3.4	0.81	92.3	n/a	156.7
					Run 6							
0.513	2.4	36.6	35.7	29.0	5.1	2.4	1.8	2.6	0.76	102.3	100.9	36.4
0.525	2.8	36.6	35.6	27.4	6.4	2.4	2.3	3.4	0.79	102.0	99	42.4
0.524	4.5	36.6	35.0	18.8	12.1	4.1	2.8	6.3	0.75	98.9	100.9	59.8
0.525	5.1	36.6	34.7	17.7	13.5	4.5	2.8	7.1	0.80	101.2	101.4	66.3
0.533	5.1	36.6	34.7	16.8	14.0	4.4	2.6	7.5	0.78	99.4	100	81.3
0.529	7.9	36.6	33.7	16.8	13.5	4.5	2.7	7.1	0.80	101.2	103.4	91.3
0.535	2.6	36.6	35.7	25.7	7.9	2.5	1.5	4.2	0.80	99.2	97.1	107.4
0.51	4.1	36.6	35.1	21.9	9.9	3.5	2.5	5.0	0.75	97.4	103.4	111.5
					Run 7							
0.296	3.6	34.9	34.3	28.6	5.4	2.5	1.8	1.6	0.95	107.3	99.2	25.7
0.294	3.9	34.9	34.5	27.2	6.5	2.9	2.1	1.9	0.88	107.5	97.9	36.0
0.303	5.2	34.9	33.5	18.9	12.9	4.1	2.1	3.9	0.89	105.3	99.4	54.9
0.303	6.1	34.9	33.5	11.7	19.2	5.0	1.7	5.8	0.88	103.9	98.3	72.1
0.314	6.9	34.9	32.3	10.8	21.8	5.8	2.5	6.9	1.01	111.5	99.3	80.4

D (h^{-1})	*Dosing*[1] (%)	S_o ($g.L^{-1}$)	$S_{o,\,adj}$[2] ($g.L^{-1}$)	*S* ($g.L^{-1}$)	*Succinic formed* ($g.L^{-1}$)	*Acetic formed* ($g.L^{-1}$)	*Formic formed* ($g.L^{-1}$)	P_{SA} ($g.L^{-1}.h^{-1}$)	Y_{SS}[3] ($g.g^{-1}$)	*% Mass accounted for*	*% Volume accounted for*[4]	*Time*[5] (h)
0.323	6.3	34.9	31.4	8.9	20.9	5.2	2.1	6.8	0.93	100.8	100.4	96.3
0.315	6.0	34.9	32.2	12.2	19.1	4.9	2.0	6.0	0.95	104.9	100.2	104.3
0.305	6.4	34.9	33.3	9.2	21.0	5.3	1.8	6.4	0.87	102.5	99	130.8
0.306	6.8	34.9	33.2	7.5	22.8	5.8	1.7	7.0	0.89	103.4	98.8	145.5
0.303	6.9	34.9	33.5	6.8	23.7	5.8	1.5	7.2	0.89	104.1	97.7	151.3
0.304	6.9	34.9	33.4	8.0	22.8	5.8	1.5	6.9	0.90	105.7	98.4	169.2
0.305	5.4	60.4	57.6	32.2	16.8	4.3	1.7	5.1	0.66	91.3	98.8	217.2
0.307	6.2	60.4	57.2	31.6	18.9	5.0	1.7	5.8	0.74	94.7	100	243.3
0.304	6.0	60.4	57.8	27.3	20.0	4.9	1.9	6.1	0.65	89.1	98.2	264.7
0.121	8.4	60.4	51.7	11.2	36.3	7.3	0.5	4.4	0.90	92.1	106.5	289.3
0.115	8.1	60.4	54.4	18.0	30.7	6.9	0.8	3.5	0.84	94.1	102.2	318.9
0.116	7.7	60.4	54.0	20.2	28.9	6.6	0.8	3.3	0.86	94.8	102.9	338.8
0.116	8.0	60.4	54.0	17.8	30.2	6.9	0.9	3.5	0.84	92.8	103.4	383.9
0.115	7.7	60.4	54.4	20.9	28.3	6.6	1.1	3.2	0.84	94.5	102.8	397.6
0.0562	8.8	60.4	50.0	11.2	36.0	7.7	0.1	2.0	0.93	94.0	107.7	418.0
0.054	9.4	60.4	52.0	10.1	36.4	8.3	0.4	2.0	0.87	92.4	105.7	439.8
0.0549	9.2	60.4	51.1	12.6	35.1	8.0	0.5	1.9	0.91	94.4	107.4	456.5
0.0549	8.8	60.4	51.1	15.1	32.6	7.7	0.8	1.8	0.91	94.4	107.1	481.1
0.048	8.9	60.4	58.5	14.9	32.8	7.8	0.8	1.6	0.75	95.0	94.8	485.3
0.0538	9.0	60.4	52.2	15.5	32.2	7.9	1.1	1.7	0.88	93.5	106.6	503.2
0.717	4.5	34.1	32.9	21.2	6.9	3.4	3.0	5.0	0.59	95.2	94.6	512.7
0.726	1.6	34.1	32.5	29.6	1.5	0.5	0.4	1.1	0.54	94.9	95.3	529.2
0.712	3.7	34.1	33.1	22.2	6.3	2.6	2.3	4.5	0.58	91.5	95	539.7

D (h^{-1})	*Dosing*[1] (%)	S_o ($g.L^{-1}$)	$S_{o,adj}$[2] ($g.L^{-1}$)	*S* ($g.L^{-1}$)	*Succinic formed* ($g.L^{-1}$)	*Acetic formed* ($g.L^{-1}$)	*Formic formed* ($g.L^{-1}$)	P_{SA} ($g.L^{-1}.h^{-1}$)	Y_{SS}[3] ($g.g^{-1}$)	*% Mass accounted for*	*% Volume accounted for*[4]	*Time*[5] (h)
0.72	5.3	34.1	32.7	17.1	11.4	4.2	3.2	8.2	0.73	96.5	94.6	554.0
0.73	4.1	34.1	32.3	20.3	8.4	3.0	2.3	6.1	0.70	94.5	95	563.3

[1] The volume percent of the total flow rate contributed by base dosing

[2] The effective glucose concentration entering the reactor based on the total flow

[3] Based on $S_{o,adj}$

[4] When deviations from the expected volumetric flow exceeded 10 %, the total expected volumetric flow, including feed, dosing and anti-foam flow rates based on pump calibrations were used to calculate D

[5] Relative to time of inoculation

III. Appendix 3

```
%This program predicts the outlet succinic acid concentration
%based on experimental acetic and formic acid values
%AA = experimental acetic acid values (g/L)
%FA = experimental formic acid values (g/L)
%SA = predicted succinic acid values (g/L)

clear all

AA=[]; % input experimental values
AA=AA./30; % convert from g/L to carbon mols
FA=[]; % input experimental values
FA=FA./46; % convert from g/L to carbon mols

V=zeros(5,length(AA)); % initialize flux distribution matrix

%v1=Glucose consumed;
%v2=SA
%v3+v4=AA;
%0.5v4=FA;

S(1,:)=[-1 0.75 1.5 1.5 0]; % node 1
S(2,:)=[0 0 1 1 -1]; % node 2
S(3,:)=[0 0 0 0 1]; %AA specified
S(4,:)=[1/3 -0.5 0.5 0 0]; % NADH balance
S(5,:)=[0 0 0 0.5 0]; %FA specified
   C(4,1)=0;
for i=1:length(AA)
       C(1,1)=0;
   C(2,1)=0;
     C(3,1)=AA(i);
     C(5,1)=FA(i)
Vnew=S\C; %solve for fluxes given a set of data points
V(:,i)=Vnew; % store flux distribution values
end
SA=V(2,:);
SA=SA';
SA=SA.*29.5 % convert from carbon mols to g/L
```

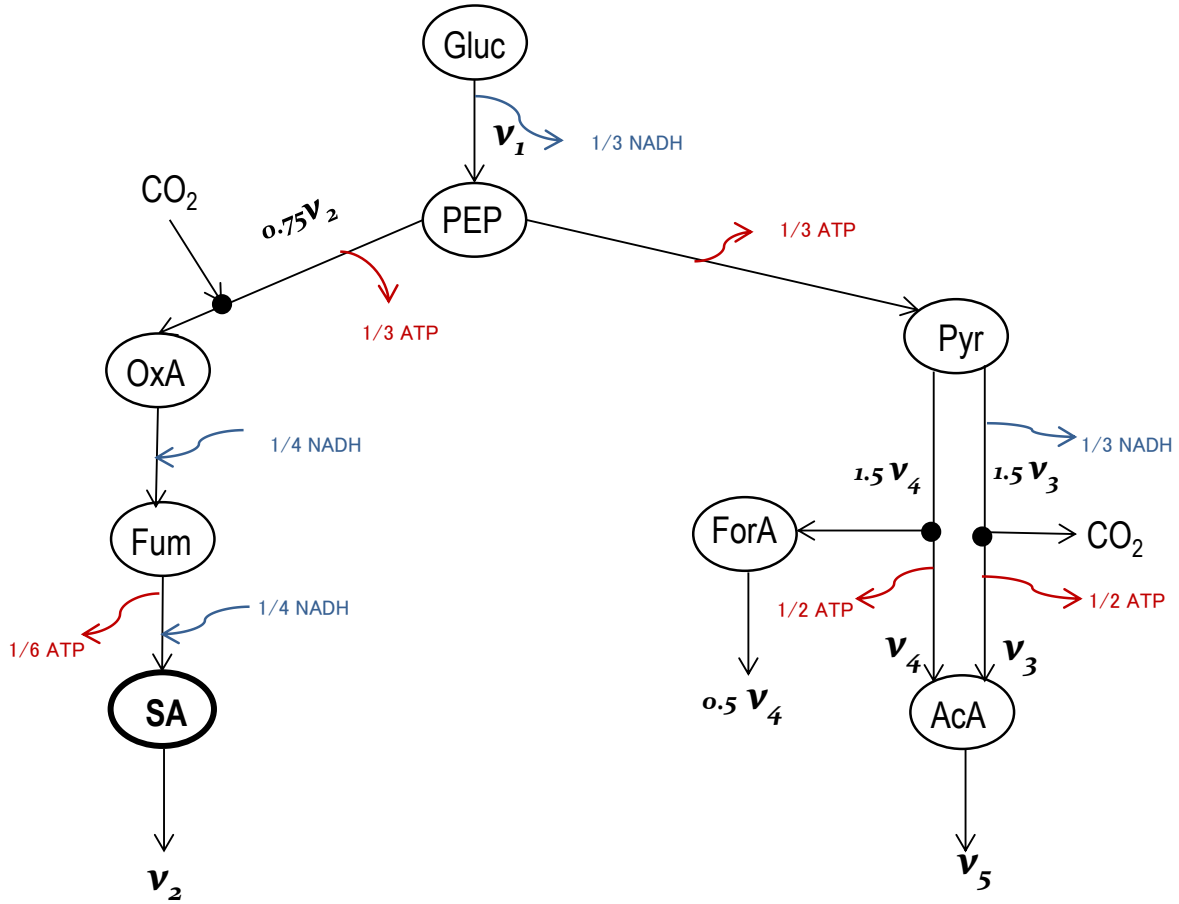

Figure III.1: *Simplified metabolic map of* Actinobacillus succinogenes *(McKinlay* et al., *2010). Only the fluxes (indicated by v_i) used in metabolic modelling have been shown. Gluc – glucose; PEP – phosphoenolpyruvate; OXA – oxaloacetate; Fum - fumarate; SA – succinate; Pyr – pyruvate; for a – formate; AcA – acetate*